

## Rapid intracellular acidification is a plant defense response countered by the brown planthopper

### Highlights

- Rapid intracellular acidification is a novel plant defense response
- Brown planthopper (BPH) delivers carbonic anhydrase (NICA) into rice for survival
- NICA counters intracellular acidification to suppress plant defense
- pH-responsive regulators of defense responses are predicted to exist in the rice-BPH interaction

### Authors

Yanjuan Jiang, Xiao-Ya Zhang, Shaoqin Li, ..., Hai-Jian Huang, Chuan-Xi Zhang, Sheng Yang He

### Correspondence

yanjuanjiang@ynu.edu.cn (Y.J.),  
chxzhang@zju.edu.cn (C.-X.Z.),  
shengyang.he@duke.edu (S.Y.H.)

### In brief

The brown planthopper (BPH) is the most devastating insect pest in rice. Jiang et al. discover that BPH secretes a salivary carbonic anhydrase (NICA) to regulate the intracellular pH of the rice cell to facilitate its feeding and survival on rice plants and that NICA counters host intracellular pH acidification to diminished defense responses.



## Article

# Rapid intracellular acidification is a plant defense response countered by the brown planthopper

Yanjuan Jiang,<sup>1,3,4,9,\*</sup> Xiao-Ya Zhang,<sup>2,3,9</sup> Shaoqin Li,<sup>4,5</sup> Yu-Cheng Xie,<sup>2</sup> Xu-Mei Luo,<sup>2</sup> Yongping Yang,<sup>4,5</sup> Zhengyan Pu,<sup>1</sup> Li Zhang,<sup>6,7</sup> Jia-Bao Lu,<sup>8</sup> Hai-Jian Huang,<sup>8</sup> Chuan-Xi Zhang,<sup>2,8,\*</sup> and Sheng Yang He<sup>3,6,7,10,\*</sup>

<sup>1</sup>State Key Laboratory for Conservation and Utilization of Bio-Resources in Yunnan, Yunnan University, Kunming 650091, China

<sup>2</sup>Institute of Insect Science, Zhejiang University, Hangzhou 310058, China

<sup>3</sup>DOE Plant Research Laboratory, Michigan State University, East Lansing, MI 48824, USA

<sup>4</sup>CAS Key Laboratory of Tropical Plant Resources and Sustainable Use, Xishuangbanna Tropical Botanical Garden, Chinese Academy of Sciences, Kunming 650223, Yunnan, China

<sup>5</sup>University of Chinese Academy of Sciences, Beijing 100049, China

<sup>6</sup>Howard Hughes Medical Institute, Duke University, Durham, NC 27708, USA

<sup>7</sup>Department of Biology, Duke University, Durham, NC 27708, USA

<sup>8</sup>State Key Laboratory for Managing Biotic and Chemical Threats to the Quality and Safety of Agro-products, Ningbo University, Ningbo 315211, China

<sup>9</sup>These authors contributed equally

<sup>10</sup>Lead contact

\*Correspondence: [yanjuanjiang@ynu.edu.cn](mailto:yanjuanjiang@ynu.edu.cn) (Y.J.), [chxzhang@zju.edu.cn](mailto:chxzhang@zju.edu.cn) (C.-X.Z.), [shengyang.he@duke.edu](mailto:shengyang.he@duke.edu) (S.Y.H.)

<https://doi.org/10.1016/j.cub.2024.09.039>

## SUMMARY

The brown planthopper (BPH) is the most destructive insect pest in rice. Through a stylet, BPH secretes a plethora of salivary proteins into rice phloem cells as a crucial step of infestation. However, how various salivary proteins function in rice cells to promote insect infestation is poorly understood. Among them, one of the salivary proteins is predicted to be a carbonic anhydrase (*Nilaparvata lugens* carbonic anhydrase [NICA]). The survival rate of the NICA-RNA interference (RNAi) BPH insects was extremely low on rice, indicating a vital role of this salivary protein in BPH infestation. We generated NICA transgenic rice plants and found that NICA expressed in rice plants could restore the ability of NICA-RNAi BPH to survive on rice. Next, we produced rice plants expressing the ratiometric pH sensor pHusion and found that NICA-RNAi BPH induced rapid intracellular acidification of rice cells during feeding. Further analysis revealed that both NICA-RNAi BPH feeding and artificial lowering of intracellular pH activated plant defense responses and that NICA-mediated intracellular pH stabilization is linked to diminished defense responses, including reduced callose deposition at the phloem sieve plates and suppressed defense gene expression. Given the importance of pH homeostasis across the kingdoms of life, discovery of NICA-mediated intracellular pH modulation uncovered a new dimension in the interaction between plants and piercing/sucking insect pests. The crucial role of NICA for BPH infestation of rice suggests that NICA is a promising target for chemical or trans-kingdom RNAi-based inactivation for BPH control strategies in plants.

## INTRODUCTION

The brown planthopper (BPH; *Nilaparvata lugens* Stål, Hemiptera, Delphacidae) is a monophagous insect pest of rice (*Oryza sativa* L.) found in all rice-growing Asian countries. The BPH sucks rice phloem sap via its stylet, causing leaf yellowing and wilting, stunted plant growth, reduced photosynthesis, and ultimately death of the rice plant.<sup>1</sup> During severe BPH outbreaks, tens of thousands of insects swarm on a rice field, resulting in the “hopperburn” phenomenon, which is characterized by large-scale wilting, yellowing, and lethal drying of rice plants.<sup>2</sup> Besides direct damage, the BPH may also indirectly damage rice plants by oviposition and transmitting viral disease agents.<sup>3,4</sup>

Application of chemical insecticides has been the main strategy for controlling BPH. Although it has the advantages of rapid killing of insects and low costs, use of insecticides leads to environmental pollution and resistance of the BPH to pesticides. In recent decades, breeding resistant rice varieties to control the BPH has attracted increasing attention. To date, more than 30 resistance genes have been found in the rice genome.<sup>5</sup> However, the BPH often quickly evolves new biological types that evade resistant rice genes. Therefore, additional methods of controlling the BPH need to be developed to complement the current control measures toward long-term solutions for achieving durable BPH resistance in rice. One method could be based on the disruption of key steps in the BPH's natural infestation process. However, development of such methods will require a



comprehensive understanding of the basic biology of BPH-rice interaction.

A critical step in the BPH's infestation of rice is the secreting of bioactive substances into the plant tissues through the stylet.<sup>6–8</sup> Specifically, during feeding, the BPH secretes both colloidal and watery saliva.<sup>9,10</sup> The main function of the colloidal saliva is to form a saliva sheath around the piercing-sucking mouthparts, stabilizing the overall feeding apparatus. The composition and function of watery saliva are more complex, and it contains salivary proteins that are believed, in most cases, to regulate various pathways in plant cells to enhance BPH feeding and survival in rice plants. For example, a salivary endo- $\beta$ -1,4-glucanase (NIEG1) degrades plant celluloses to help the BPH's stylet reach the phloem<sup>11</sup>. NISEF1, an EF-hand (a motif that consists of an  $\alpha$ -helix “E,” a loop that may bind calcium, and a second  $\alpha$ -helix “F”)  $\text{Ca}^{2+}$ -binding protein, interferes with calcium signaling and  $\text{H}_2\text{O}_2$  production during BPH feeding.<sup>12</sup> Salivary protein 7 is required for normal feeding behavior and for countering accumulation of a defense compound, tricin.<sup>13</sup> On the other hand, a BPH mucin-like protein (NIMLP) triggers defense responses in rice cells, including cell death, callose deposition, and upregulation of pathogen-responsive genes.<sup>14,15</sup>

Carbonic anhydrases (CAs) (Enzyme Commission 4.2.1.1) are zinc metalloenzymes that function as catalysts in the bidirectional conversion of  $\text{CO}_2$  and water into bicarbonate and protons.<sup>16</sup> There are at least five distinct CA families ( $\alpha$ -,  $\beta$ -,  $\gamma$ -,  $\delta$ -, and  $\epsilon$ -CAs), and three of them ( $\alpha$ -,  $\beta$ -, and  $\gamma$ -CAs) are ubiquitously distributed among animal, plant, and bacterial species. The widespread distribution and adequate abundance of these CA families underline their evolutionary importance throughout the kingdoms of life. CAs participate in a wide range of biological processes, such as pH regulation,  $\text{CO}_2$  homeostasis, stomatal aperture, and plant defense.<sup>17–21</sup> NICA belongs to the  $\alpha$ -CA subfamily. Our previous study showed that *Nilaparvata lugens* carbonic anhydrase (NICA) is expressed in BPH salivary glands.<sup>6</sup> Surprisingly, however, RNA interference (RNAi) of the NICA transcript in BPH insects affects neither pH maintenance within the insect salivary gland, watery saliva or gut, nor insect feeding behavior or honeydew excretion on artificial diet, but greatly reduced survival of BPH on rice plants, suggesting a critical function *in planta* via an unknown mechanism.<sup>6</sup>

Here, we report that NICA-RNAi BPH feeding results in rapid intracellular acidification of rice cells. We found that NICA is secreted into the rice tissues during BPH feeding and functions as an effector that stabilizes host cell intracellular pH, accompanied by suppression of defense responses. Thus, we have uncovered intracellular pH homeostasis as a previously uncharacterized battleground in plant-insect interactions.

## RESULTS

### NICA is detected in rice sheath tissues during BPH feeding

NICA was previously found to be highly expressed in salivary glands and present in the watery saliva of BPH fed on an artificial diet.<sup>6</sup> We conducted a more detailed characterization of NICA expression in this study. RNA *in situ* hybridization showed that the expression level of NICA was detectable throughout the principal glands (PGs) and accessory glands (AGs), but not in

A-follicle of the PG (APG) (Figure 1A), which further raised the possibility that NICA may be one of the “effector proteins” secreted into the rice tissue during BPH feeding on rice plants. To test this possibility, we compared protein profiles in the leaf sheaths of Nipponbare rice plants before and after BPH feeding using liquid chromatography-mass spectrometry (LC-MS). We found 8 NICA-specific peptides in BPH-fed leaf sheath tissue (Figure 1B; Table S1), confirming that NICA is secreted into the host tissues during BPH feeding. As BPH is a phloem-feeding insect, its effector proteins, such as NICA, presumably act in the phloem. We therefore collected the phloem exudate from Nipponbare rice leaf sheaths, with or without BPH feeding, for LC-MS analysis (Figure 1C). Six NICA-specific peptides were detected in the phloem exudate of Nipponbare plants that had been fed on by BPH (Figure 1B), demonstrating that NICA is delivered into phloem by BPH.

### Transgenic expression of NICA in rice rescues the ability of NICA-silenced BPH to feed and survive

To further clarify the site of function (i.e., in insect vs. in plant) of NICA in the BPH-rice interaction, we produced transgenic Nipponbare plants expressing NICA (see STAR Methods). A total of 26 lines were produced, and 6 lines were found to robustly express the NICA transcript (Figure S1A). NICA-expressing plants exhibited no noticeable changes in appearance compared with Nipponbare plants (Figures S1B–S1D). NICA-expressing plant lines were propagated to T3 generation, and three lines were subjected to further characterization, including BPH feeding. For BPH feeding assay, double-stranded RNA (dsRNA) of NICA (dsNICA) or the control green fluorescent protein gene (dsGFP) was injected into 3<sup>rd</sup> instar BPH nymphs to initiate RNAi of the NICA transcript.<sup>22</sup> Quantitative real-time PCR analysis confirmed that the transcript levels of the NICA gene were reduced by 99% and 97%, respectively, in tested individuals when compared with non-RNAi control and dsGFP-treated insects (Figure 2A). There were no significant differences in the survival rates between dsGFP and dsNICA BPH when fed on the artificial diet, indicating that silencing NICA expression has no obvious impact on the basic physiology of BPH (Figure 2B). However, we found that the survival rate of dsNICA BPH was sharply decreased, starting at day 9 post infestation, to ~40% at day 14, whereas the control dsGFP BPH survived normally on wild-type (WT) Nipponbare plants (Figure 2C). This result is consistent with previous results conducted in the *japonica* cultivar Xiushui134 rice plants,<sup>6</sup> suggesting that the requirement of NICA for BPH survival is not specific to a specific rice genotype. Strikingly, NICA transgenic plants almost fully restored the survival of NICA-silenced BPH insects (Figure 2C; Figures S1E and S1F), demonstrating that NICA expressed in the host tissue (Figures 2D and 2E) can complement the infestation defect of NICA-silenced BPH insects.

### The conserved catalytic site amino acids of NICA are critical to its function in rice

NICA contains several conserved amino acid residues predicted to be at the catalytic site of CAs (Figure 2F). We asked whether some of these conserved active site residues are critical to the function of NICA in rice-BPH interaction. Accordingly, we expressed three different NICA mutants in Nipponbare

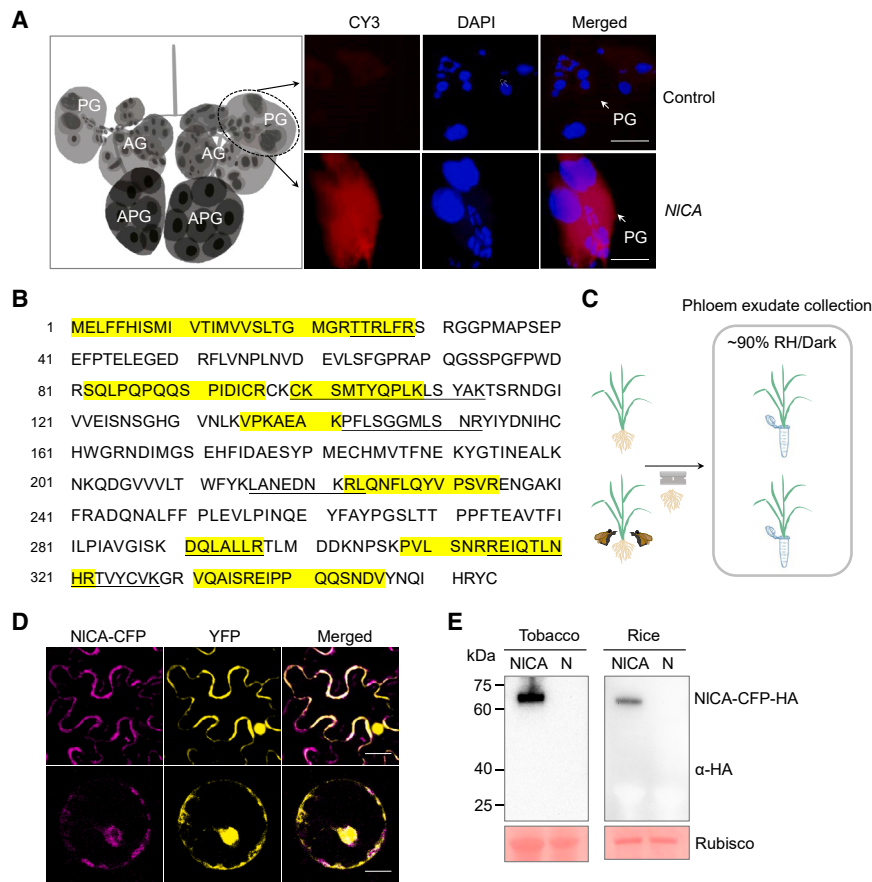


**Figure 1. Initial characterization of *Nilaparvata lugens* carbonic anhydrase (NICA)**

(A) *In situ* RNA hybridization of salivary glands in 5-instar BPHs. Left, a schematic diagram of BPH salivary glands, including the principal glands (PGs), the accessory glands (AGs), and the A-follicle of the principle gland (APG). Right, NICA expression was detectable in the PG (red) using antisense NICA sequence as a probe. Sense NICA probe was used as a negative control. Nuclei are stained blue by 4',6-diamidino-2-phenylindole (DAPI). Scale bar, 50  $\mu$ m.

(B) The amino acid sequence of NICA. The highlighted amino acid residues indicate the peptides detected in BPH-infested rice sheath tissue by LC-MS analysis. The underlined amino acid residues indicate the peptides detected in phloem exudate of BPH-infested rice by LC-MS analysis.

(C) A schematic diagram of the phloem exudate collection.

(D) NICA is colocalized with the YFP signals in *N. benthamiana* (upper row; scale bar, 10  $\mu$ m) and rice cells (lower row; scale bar, 5  $\mu$ m). YFP and NICA-CFP fusion proteins were co-expressed in *N. benthamiana* leaf cells for 48 h using the *Agrobacterium*-mediated transient expression method. YFP and NICA-CFP fusion proteins were co-expressed in rice protoplasts 16 h after the corresponding DNA constructs were introduced into rice protoplasts via polyethylene glycol-mediated transformation. Experiments were repeated three times with similar trends.

(E) NICA-CFP-hemagglutinin (HA) fusion protein levels are detected with anti-HA (Zenbio, 301113) in *N. benthamiana* leaves and rice protoplasts.

Protein samples were extracted from NICA-CFP-HA-expressing *N. benthamiana* and rice protoplasts. Proteins from mock *N. benthamiana* leaves and rice protoplasts were as negative controls (N). Ponceau S staining of Rubisco shows protein loading control. See also Figure S5 and Table S1.

plants (Figures S1A and S1G). “NICA-*m1*” plants contain a NICA transgene in which His<sup>159</sup> and His<sup>161</sup> were mutated to Ala; “NICA-*m2*” plants contain a NICA transgene in which Glu<sup>182</sup> and His<sup>184</sup> were replaced by Ala; and “NICA-*m3*” plants carry a NICA transgene in which all seven conserved active site residues, His<sup>159</sup>, His<sup>161</sup>, Glu<sup>171</sup>, Glu<sup>182</sup>, His<sup>184</sup>, Thr<sup>269</sup>, and Phe<sup>279</sup>, were changed to Ala. Like NICA transgenic plants, transgenic plants expressing these NICA mutants exhibited no noticeable changes in appearance (Figures S1B–S1D). We conducted BPH survival assay and found that in contrast to plants expressing WT NICA, the NICA-*m2* and NICA-*m3* plants could not fully rescue the infestation defect of NICA-silenced BPH insects. The NICA-*m1* plants, on the other hand, could recover the infestation defect of dsNICA BPH (Figures 2G and 2H; Figure S2). Thus, the conservative residues Glu182 and His184 and possibly some other residues at the predicted catalytic site are indispensable for the function of NICA inside the plant cell.

After showing the requirement of catalytic site residues for the function of NICA in rice, we next investigated the subcellular localization of NICA in both *Nicotiana benthamiana* leaf cells and rice leaf protoplasts transiently expressing cyan fluorescent protein (CFP) fused NICA:CFP. In both cases, NICA:CFP showed a nonuniform distribution of CFP signal in the cell. Further colocalization studies with YFP signal revealed that NICA was

predominantly localized in the cytoplasm (Figure 1D). There was some nuclear localization of NICA-CFP in rice protoplasts. Intact NICA:CFP proteins were detected in these localization experiments (Figure 1E).

### NICA counters rapid intracellular acidification during BPH feeding on rice

BPH feeding on rice plants can be divided into two phases, based on electropetrography (EPG) waveforms.<sup>23</sup> The first phase involves BPH’s stylet penetrating the plant through the cell walls and cell membranes of various epidermal and mesophyll cells until the stylet reaches the phloem sieve cells inside the vascular system. In Nipponbare, the time to reach the phloem sieve cells can be around 1.2 h before sustained phloem sap ingestion occurs at 3.8 h.<sup>23</sup> Our finding of the site of NICA action in the plant prompted us to test the hypothesis that NICA might modulate rice cell pH changes during BPH feeding. To directly test this hypothesis, we constructed a rice transgenic line expressing a cytoplasmic ratiometric pH sensor driven by the 35S promoter, cyto-pHusion. Cyto-pHusion consists of the tandem concatenation of enhanced green fluorescent protein (EGFP) and a monomeric red fluorescent protein 1 (mRFP1).<sup>24</sup> EGFP is highly sensitive to pH variation, with the brightest EGFP signal emitted at a pH of 7–8. EGFP fluorescence is gradually quenched at lower pH values and totally quenched at pH

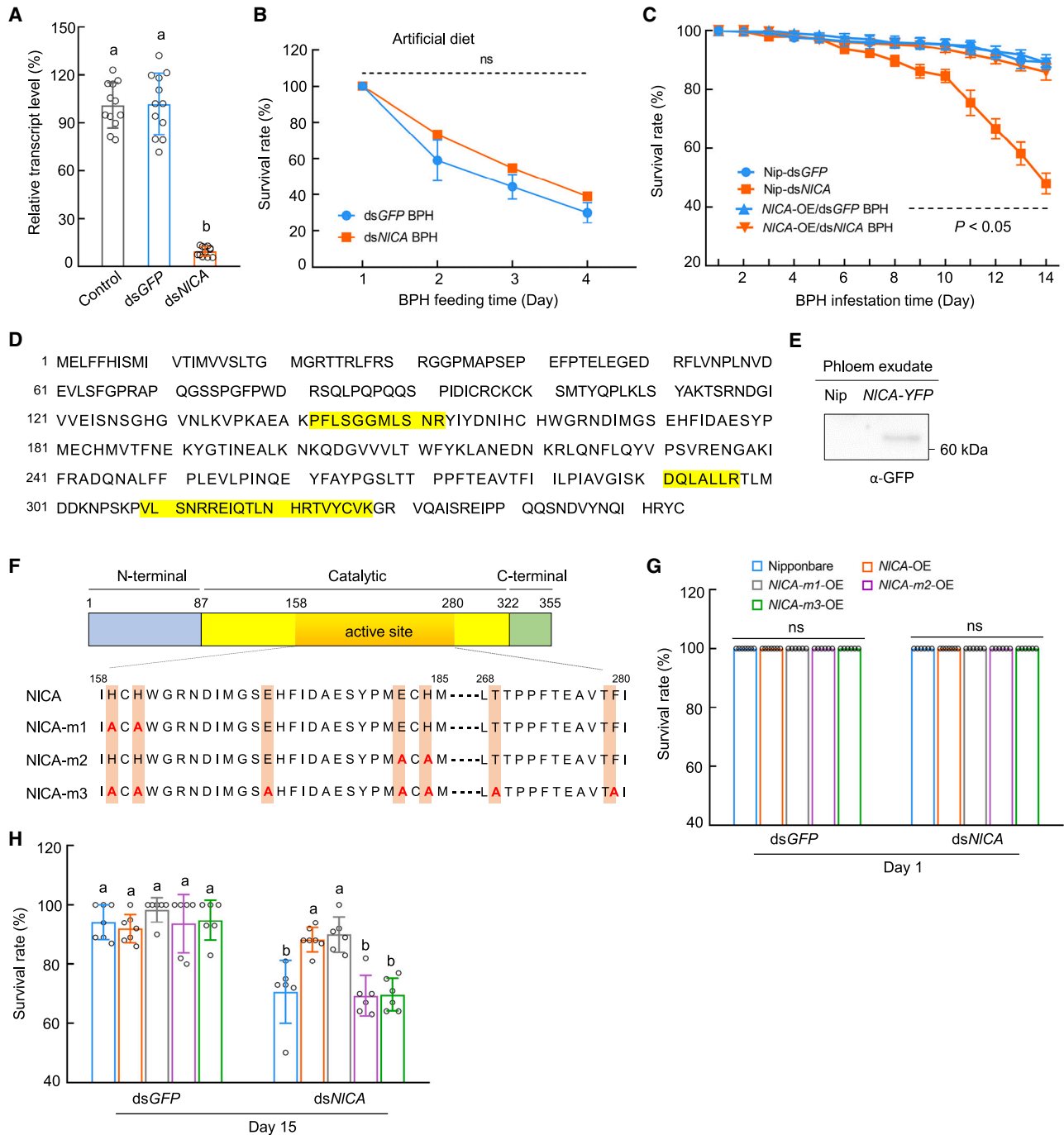


**Figure 2. Effects of NICA RNAi on BPH survival on rice cultivar Nipponbare**

(A) The NICA transcript levels in BPH at 3 days post injection of dsGFP or dsNICA were determined by quantitative real-time PCR (displayed as % of the NICA transcript abundance in control BPH). Values are displayed as mean  $\pm$  SEM of 4 experimental replicates (two-way ANOVA; 3 biological replicates in each experiment and 30 individual insects pooled for each biological replicate).

(B) The daily survival rates of dsNICA-injected BPH insects feeding on artificial diet. Values are displayed as mean  $\pm$  SEM of 3 biological replicates (1 biological replicate includes 50 individual BPH adults fed on artificial diet in a lucifugal plastic bottle).

(C) The daily survival rates of dsNICA-injected BPH insects feeding on Nipponbare (Nip) and NICA-expressing line 1. Values are displayed as mean  $\pm$  SEM of 8 biological replicates (two-way ANOVA; 20 individual 2nd BPH nymphs per rice plant for each biological replicate). The black dashed line indicates significant differences ( $p < 0.05$ ) in survival rates starting from day 9 between dsNICA BPH on Nip and other treatments.

(D) The amino acid sequence of NICA. The highlighted amino acid residues indicate the peptides detected in the phloem exudate of NICA-OE transgenic rice plants by LC-MS analysis.

(legend continued on next page)

values < 5. In contrast, mRFP1 is insensitive to pH changes in the physiologically relevant range and serves as an internal reference. We placed 5<sup>th</sup> instar BPH nymphs on the leaf sheath of cyto-pHusion-expressing rice plants and recorded GFP and RFP signals of the feeding sites under microscopic observation at different time points with a 12-h test period. BPH can move around from one feeding site to another during the 12-h feeding experiments. The average feeding time at a feeding site is around 8 h. Therefore, the first 8 h of cellular responses best capture mostly synchronized rice-BPH interactions at a typical feeding cycle. As shown in Figures 3A–3D, dsNICA BPH feeding induced a significant pH decrease in the phloem sieve elements/companion cells at 4 and 8 h (Figures 3C and 3D). The decreased ratio of EGFP:mRFP was caused by the quenched EGFP signals after dsNICA BPH feeding, while the internal control, mRFP, kept at a stable level (Figures S3A–S3H). By contrast, dsGFP BPH feeding did not elicit an obvious intracellular pH change in the phloem sieve elements/companion cells during this period. These results uncovered a previously uncharacterized plant cellular response—rapid intracellular acidification—during the early stage of dsNICA BPH feeding and demonstrated that BPH has evolved a critical virulence effector, NICA, to counter this novel plant cellular response. Interestingly, we noted that the control dsGFP WT BPH feeding induced slight intracellular acidification at 12 h (Figure 3E). At this late time point of feeding, most BPHs would have left their initial feeding sites and have relocated to new feeding sites. In our analysis, we could not distinguish between old and new feeding sites. It is therefore likely that active BPH feeding (i.e., active NICA injection) is needed to maintain intracellular pH homeostasis at all feeding sites.

Next, we conducted experiments to determine whether intracellular acidification is a highly localized cell-type-specific response or a spreading local response. We imaged and calculated the intracellular pH in the mesophyll cells and epidermal cells at the feeding site. We found that intracellular acidification occurred in the mesophyll cells and epidermal cells (Figures S3I–S3L) in response to feeding by dsNICA BPH, albeit to a lesser degree compared with that in the sieve elements/companion cells. In contrast, rice plants fed on by dsGFP WT BPH responded with an initial slight intracellular acidification at 1.5 h but then consistently maintained a more alkalized intracellular pH in the mesophyll and epidermal cells compared with non-fed rice plants and dsNICA BPH (Figures S3I–S3L).

Because extracellular pH change is associated with plant responses to biotic stress,<sup>25,26</sup> we speculated that rapid intracellular acidification of dsNICA BPH feeding might induce defense gene expression. To test this possibility, Nipponbare plants infested by dsGFP and dsNICA BPH were examined for defense gene expression. Commonly used marker genes (e.g., *OsNH1*, *OsNH2*, *OsWRKY45*, and *OsWRKY13*) in the studies of rice

defense against BPH were selected.<sup>27–30</sup> We found that expression of those genes was significantly induced at a higher level by dsNICA BPH infestation than by dsGFP BPH control at 4 and 8 h (Figures 3F–3I), which is consistent with the intracellular pH change at 4 and 8 h (Figures 3C and 3D). These results indicate that intercellular acidification is linked to rice defense activation.

### Ectopic intracellular acidification causes defense gene expression in rice plants

Because plant defense responses are important for limiting BPH survival in rice,<sup>28,31–33</sup> we conducted experiments to determine whether intracellular acidification would trigger defense gene expression. Rice is normally grown in Yoshida medium, pH of 4.<sup>34</sup> To test whether medium pH changes can modulate defense responses in rice, we first grew rice seedlings in Yoshida medium until they reached the 5-leaf stage and then placed them in fresh Yoshida medium with pH adjusted to 2, 3, 4, 5, 6, and 7, respectively, for 48 h. Interestingly, drastically increased expression of defense response genes (e.g., *OsNH1*, *OsNH2*, *OsWRKY45*, and *OsPBZ1*) was observed in Nipponbare plants at an acidic pH of 2 (Figures S4A–S4H). The pHusion sensor plants exposed to external pH of 2 showed intracellular acidification that simulates pH changes observed during BPH feeding (Figures 3J–3K). Survival rates of BPH insects were lower in Nipponbare plants growing in media with a pH of 2 compared with those growing in media with a pH of 4 (Figure 3L). These results suggest that cellular acidification is sufficient to induce defense gene expression in rice and to reduce BPH's ability to survive on rice.

### Rice defense responses are inhibited by NICA

As NICA stabilizes intracellular pH during WT BPH feeding (Figures 3A–3D), and both dsNICA BPH feeding and ectopic intracellular acidification cause activation of defense gene expression (Figures 3F–3I; Figure S4), we next tested the hypothesis that a major function of NICA-mediated stabilization of intracellular pH may be to prevent over-stimulation of downstream rice defense responses during feeding. Callose deposition in the phloem sieve tubes is a classical defense response that is associated with the feeding of piercing-sucking insects.<sup>35</sup> We examined this response using aniline blue to stain callose in the phloem sieve cells. Indeed, fewer and smaller callose depositions were found in the sieve plates of NICA-expressing leaf sheaths compared with those found in the sieve plates of Nipponbare (Figures 4A–4H) at 72 h after BPH feeding, demonstrating that NICA suppresses callose deposition in sieve cell plates. Furthermore, dsNICA BPH induced higher expression of callose biosynthesis genes, such as *OsGSL1*, *OsGSL3*, *OsGLS5*, and *OsGns5*, than the dsGFP control BPH; however, the induction of these genes was greatly compromised in NICA transgenic

(E) Yellow fluorescent protein (YFP) fused NICA protein (NICA-YFP) is detectable in the phloem exudate of NICA-OE transgenic plants by anti-GFP antibody (Abmart, 20004).

(F) Schematic display of the NICA protein with the N terminus displayed in blue, the C terminus in green, and the central catalytic domain in yellow/orange. The amino acid (aa) sequence (158–280 aa) of the putative active site is showed. Amino acid substitutions in NICA-m1, NICA-m2, and NICA-m3 are indicated in red.

(G and H) The survival rates of 20 dsGFP and dsNICA BPH insects in Nip and NICA transgenic plants after 1 day (G) and 15 days (H) post infestation. Values are displayed as mean ± SEM ( $n \geq 6$  biological replicates; 20 individual 2<sup>nd</sup> BPH nymphs per rice plant for each biological replicate). ns indicates no significant difference between treatments (two-way ANOVA). Different letters indicate statistically significant differences analyzed by two-way ANOVA (Tukey test,  $p < 0.05$ ). Experiments were repeated three times with similar trends. See also Figures S1 and S2.

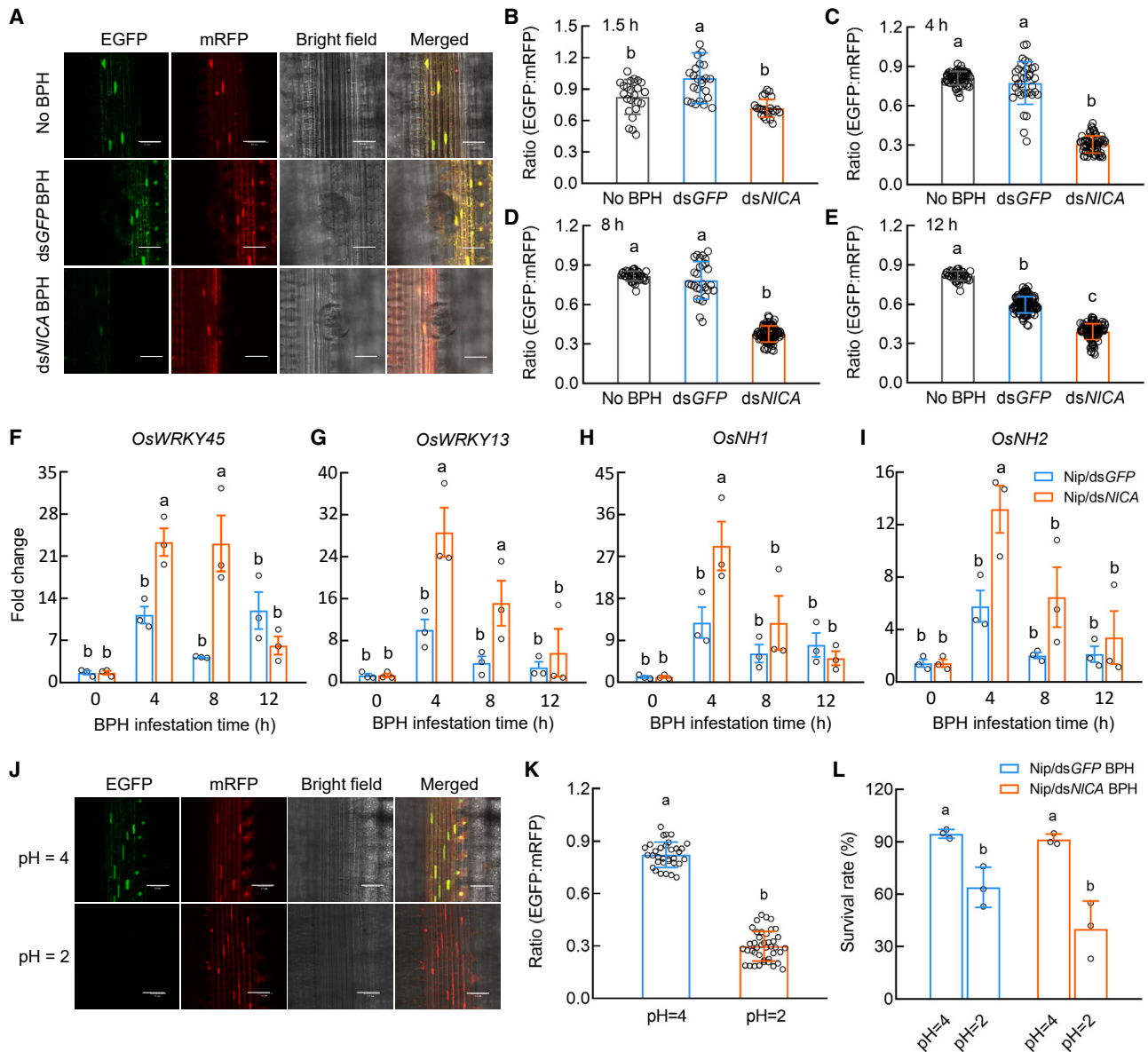


**Figure 3. Role of NICA in maintaining intracellular pH of rice cells**

(A) Confocal microscopic images at BPH feeding sites in Nipponbare plants expressing a ratiometric cytoplasmic pH sensor (cyto-pHusion) 4 h after placing 30 5<sup>th</sup>-instar BPH nymphs on each plant. A 40.0 $\times$  objective was used to capture every feeding site on the tiled 1  $\times$  1 cm section of rice leaf sheath. Confocal images from plants with no BPH feeding served as the control. Scale bar, 20  $\mu$ m.

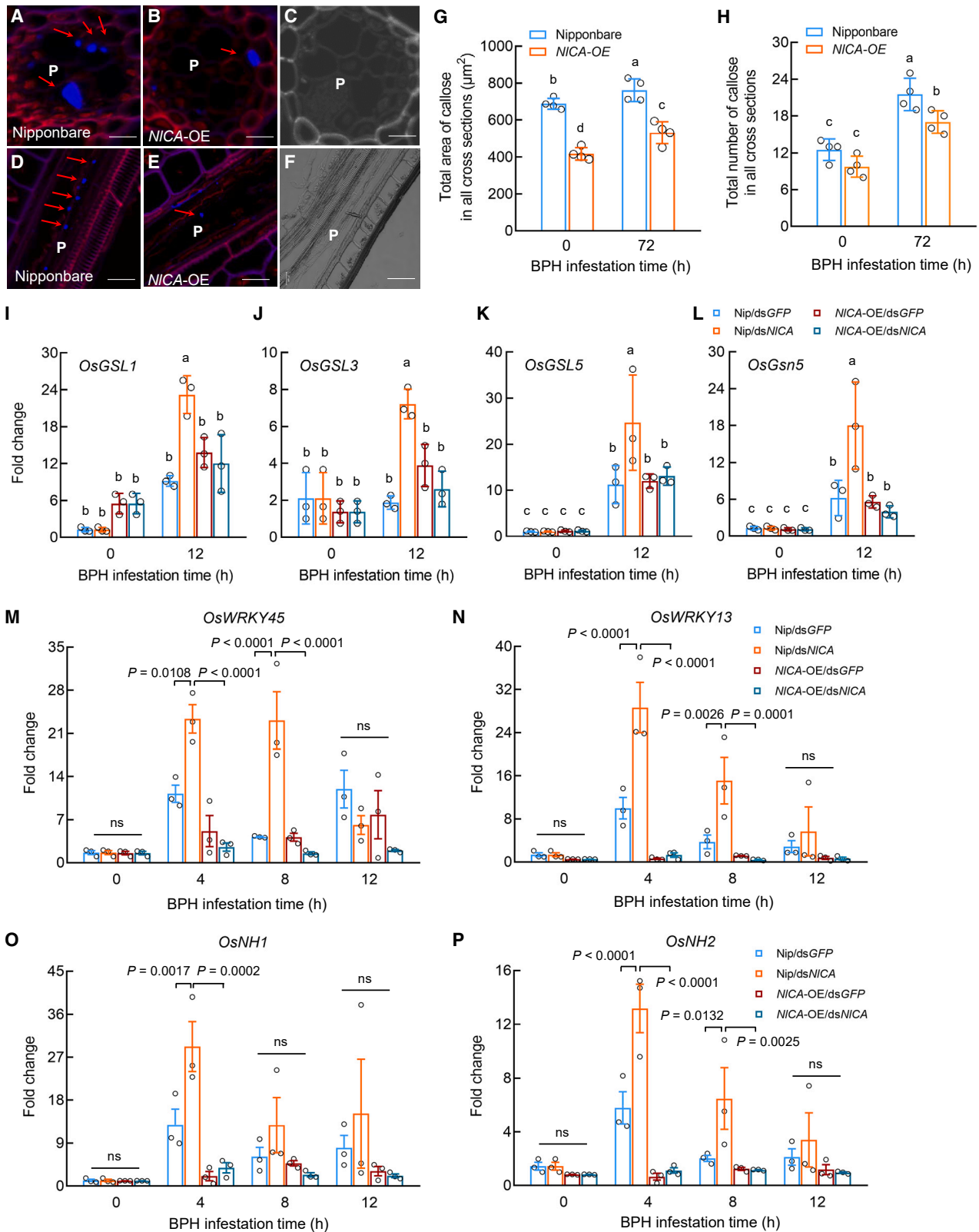
(B–E) EGFP:mRFP signal ratios at 1.5 (B), 4 (C), 8 (D), and 12 h (E) of dsGFP or dsNICA BPH treatment compared with no BPH control. EGFP was imaged at  $\lambda_{Ex}$  = 500 nm and  $\lambda_{Em}$  = 540 nm. mRFP was imaged at  $\lambda_{Ex}$  = 570 nm and  $\lambda_{Em}$  = 620 nm. Values are displayed as mean  $\pm$  SEM ( $n \geq 24$  circular areas of leaf sheath phloem with a diameter of 100  $\mu$ m, with the feeding site at the center).

(F–I) Expression of defense response genes, *OsWRKY45* (F), *OsWRKY13* (G), *OsNH1* (H), and *OsNH2* (I), in Nipponbare plants infested by dsGFP or dsNICA BPH. Values are displayed as mean  $\pm$  SEM of three biological replicates. Each biological replicate represents pooled leaf sheaths from three individual rice plants fed on by 20 5<sup>th</sup> instar BPH nymphs per plant.

(J) Confocal microscopic images of Nipponbare plants expressing a ratiometric cytoplasmic pH sensor (cyto-pHusion) at 12 h after being transferred to Yoshida medium at a pH of 2. Confocal images from plants grown in Yoshida medium with a pH of 4 served as the control. Scale bar, 15  $\mu$ m.

(K) EGFP:mRFP signal ratios. EGFP was imaged at  $\lambda_{Ex}$  = 500 nm and  $\lambda_{Em}$  = 540 nm. mRFP was imaged at  $\lambda_{Ex}$  = 570 nm and  $\lambda_{Em}$  = 620 nm. Values are displayed as mean  $\pm$  SEM ( $n \geq 33$  calculation area per condition).

(L) The 7<sup>th</sup>-day survival rates of dsGFP- and dsNICA-injected BPH insects feeding on Nipponbare growing in media with different pHs. Values are displayed as mean  $\pm$  SEM of 3 biological replicates (20 individual insects per biological replicate). Different letters indicate statistically significant differences analyzed by two-way ANOVA (Tukey test,  $p < 0.05$ ). Experiments were repeated three times with similar trends. See also Figures S3 and S4.



(legend on next page)



plants, with or without BPH treatment (Figures 4I–4L). We also measured the transcript levels of defense marker genes (e.g., *OsNH1*, *OsNH2*, *OsWRKY45*, and *OsWRKY13*) in Nipponbare and *NICA*-expressing plants that had been fed on by *dsGFP* and *dsNICA* BPH. As shown in Figures 4M–4P, induced expression of *OsNH1*, *OsNH2*, *OsWRKY13*, and *OsWRKY45* by *dsNICA* BPH was suppressed in *NICA* transgenic plants compared with those in Nipponbare plants. Collectively, these results showed that *NICA*-mediated intracellular pH homeostasis is linked to downregulation of callose deposition in phloem sieve cells as well as defense gene expression in rice plants.

## DISCUSSION

In this study, we provided evidence that intracellular acidification is a previously unrecognized plant defense response that occurs during BPH feeding on rice. This finding was facilitated by our attempt to understand the role of *NICA* in rice–BPH interaction. We found that the *NICA* transcript is detected mainly in the salivary glands (Figure 1A) and that the *NICA* protein is found in rice tissues, including the phloem sap, that have been fed on by BPH (Figure 1B). *NICA*-silenced (*dsNICA*) insects survived very poorly on at least two independent cultivars of rice plants, Xiushui134<sup>6</sup> and Nipponbare (Figure 2), whereas *NICA*-expressing rice plants can restore the normal survival of *NICA*-silenced (*dsNICA*) insects (Figure 2; Figure S1), suggesting that *NICA* functions in plant cells. Using the cytoplasm pH sensor, we found that *NICA* is required for BPH to maintain a normal plant cytoplasm pH during BPH feeding (Figures 3A–3D; Figure S3). Pathogen/insect-derived effectors can be powerful molecular probes for discovering novel plant regulators/responses to biotic attacks. Although other piercing/sucking herbivore-derived effectors, such as Btfer1, LsPDI1, LsSP1, Mp55, DNase II, and BISP, have been reported as defense-suppressive effectors,<sup>36–41</sup> our discovery of intracellular acidification as a plant defense response and our finding that BPH secretes *NICA* as a counter-defense measure show host cell pH homeostasis as a novel battlefield that has not been revealed in any plant-biotic interactions.

Extracellular alkalinization of cultured plant cells has long been recognized as a canonical plant response to microbial elicitors as well as endogenous plant signals.<sup>26</sup> Extracellular alkalinization caused by plant endogenous RAPID ALKALINIZATION FACTOR (RALF) peptides, for example, is perceived by the

FERONIA-family receptors.<sup>42,43</sup> There is evidence that this perception causes phosphorylation of plasma membrane (PM)-localized H(+)-ATPase 2, resulting in the inhibition of proton transport across the PM.<sup>44</sup> Notably, extracellular alkalinization has recently been shown to inhibit or promote growth- or immunity-associated cell-surface-receptor functions through specific pH-sensitive amino acid sensors.<sup>26</sup> In contrast, defense regulation by intracellular pH changes had escaped the discovery of researchers until this study. Our demonstration of a link between intracellular acidification and defense activation has laid a foundation for the future discovery of potentially diverse pH-sensitive intracellular regulators of defense responses, which could add a new dimension to the study of plant-biotic interactions.

Because cellular pH alterations could potentially affect multiple biomolecules and, hence, multiple cellular processes, future research should comprehensively define all cellular processes that are affected by intracellular pH acidification. In this study, we found that this pH change is linked to activation of callose deposition at phloem sieve cells and expression of defense response genes, such as *OsNH1*, *OsNH2*, *OsPBZ1*, and *OsWRKY45* (Figure 3; Figure S4). Conversely, *NICA*-mediated intracellular pH stabilization dampens these defense responses (Figure 4). Callose deposition in phloem sieve cells, in particular, is a classical defense response to a variety of sucking/piercing insects and is thought to limit nutrient flow during insect feeding.<sup>35,45–48</sup> Together, these results suggest that a major effect of *NICA*-mediated pH stabilization is to prevent overactivation of defense responses during BPH feeding.

The mechanism by which *NICA* counters intracellular acidification is likely inherent in its reversible inter-conversion of carbon dioxide and water into carbonic acid, protons, and bicarbonate ions. CAs are universally present in all organisms (Figure S5); other piercing/sucking insects may use CAs or another mechanism to manipulate host intracellular pH as part of their infestation strategy. Indeed, CA has been reported as a protein component of saliva in rice green leafhopper, *Nephotettix cincticeps*,<sup>49</sup> and aphid *Myzus persicae*.<sup>50</sup> In the case of *M. persicae*, CA-II was shown to increase viral transmission via plant apoplastic-acidification-mediated acceleration of intracellular vesicular trafficking.<sup>50</sup> However, because *NICA* plays a critical role in BPH's survival on rice plants per se (i.e., in the absence of viral infection), as shown in this study, it is likely that insect-secreted CAs play a primary role in facilitating insect survival by countering intracellular-acidification-associated

### Figure 4. *NICA* dampens callose deposition and defense gene expression

(A–F) Callose accumulation (bright blue fluorescence indicated by red arrows) on the sieve plates of Nipponbare leaf sheaths (A and D) and *NICA*-OE leaf sheaths (B and E) plants at 72 h after BPH feeding. P, phloem. The pictures were taken under a Zeiss microscope. (A and B) Cross-sections. Scale bar, 5  $\mu$ m. (D–E) Longitudinal sections. Scale bar, 10  $\mu$ m. (C and F) The bright-field views of cross and longitudinal phloem sections, respectively. (G) Total areas of callose deposition in BPH-infested leaf sheaths of Nipponbare and *NICA*-OE. Each data point represents the total areas of callose deposition found in 300 cross-sections of each experiment. Values are displayed as mean  $\pm$  SEM of four experiments. (H) Total number of callose deposits in BPH-infested leaf sheaths of Nipponbare and *NICA*-OE. Each data point represents the total number of callose deposits found in 300 cross-sections of each experiment. Values are displayed as mean  $\pm$  SEM of four experiments. (I–L) Relative expression levels of the callose synthase genes *OsGSL1* (I), *OsGSL3* (J), *OsGSL5* (K), and *OsGns5* (L) in response to BPH feeding. Values are displayed as mean  $\pm$  SEM of 3 biological replicates. Each biological replicate represents pooled leaf sheath from 3 individual rice plants fed on by 20 5<sup>th</sup> instar BPH nymphs per plant. (M–P) Expression of defense marker genes *OsWRKY45* (M), *OsWRKY13* (N), *OsNH1* (O), and *OsNH2* (P) in response to BPH feeding. Values are displayed as mean  $\pm$  SEM of 3 biological replicates. Each biological replicate represents pooled leaf sheaths from 3 individual rice plants fed on by 20 5<sup>th</sup> instar BPH nymphs per plant. ns indicates no significant difference between treatments (two-way ANOVA). Different letters indicate statistically significant differences analyzed by two-way ANOVA (Tukey test,  $p < 0.05$ ). Experiments were repeated three times with similar trends.

defense activation. Future research could examine whether CA-mediated increases in viral transmission may be affected by defense suppression.

Discovering the role of pH regulation during plant response to biotic and abiotic stresses and characterizing the impact of such pH alterations could be an important area for future research. Because maintaining proper external and internal pH is critical for all forms of life, prokaryotic and eukaryotic organisms alike have evolved mechanisms to achieve pH homeostasis. Facing fluctuating external pH, prokaryotes have evolved diverse mechanisms for sensing external pH. For instance, the bimodal sensing of pH is employed by *Bacillus subtilis* and *Escherichia coli*.<sup>51</sup> Fungi employ a conserved pathway, mediated by Rim101 and PacC, to sense external pH.<sup>52</sup> It has been reported that different subcellular compartments within the plant cell maintain different pH values, presumably as part of carrying out their unique physiological functions.<sup>53</sup> The demonstrated ability of NICA to counter stimulus-dependent pH changes in plant cells could make NICA a useful molecular tool to modulate and broadly understand the effects of pH stabilization on plant signaling and metabolic pathways in different cell types, organelles, and tissues in plants by, for example, targeting NICA expression in specific tissues, cells, or organelles. Additionally, the crucial role of NICA for BPH infestation of rice suggests that NICA is an important target for chemical or trans-kingdom RNAi-based inactivation for the development of novel BPH control strategies in plants.

## RESOURCE AVAILABILITY

### Lead contact

Further information or requests for resources and reagents should be directed to and will be fulfilled by the lead contact, Sheng Yang He ([Shengyang.he@duke.edu](mailto:Shengyang.he@duke.edu)).

### Materials availability

All novel materials described in this paper will be made available upon request, subject to completion of an MTA.

### Data and code availability

- All data reported in this paper will be shared by the [lead contact](#) upon request.
- No original code is reported in this paper.
- Additional information required to reanalyze the data reported in this paper is available from the [lead contact](#) upon request.

## ACKNOWLEDGMENTS

We thank our lab member, Richard Hilleary, for his comments and suggestions during this work. This study was supported by funding from the Natural Science Foundation of China (32360082 and 31870259, which supported Y.J.'s research at Michigan State University); the Yunnan Fundamental Research Projects (202401AS070122 and 202105AC160028) to Y.J.; Zhejiang University (which supported the research of X.-Y.Z. at Michigan State University); Howard Hughes Medical Institute to S.Y.H.; and the National Key Research and Development Plan in the 14<sup>th</sup> five-year plan (2021YFD1401100) to C.-X.Z.

## AUTHOR CONTRIBUTIONS

S.Y.H., C.-X.Z., Y.J., and X.-Y.Z. conceptualized and designed this study. Y.J., X.-Y.Z., S.L., Y.-C.X., X.-M.L., Y.Y., Z.P., L.Z., J.-B.L., and H.-J.H. performed experiments and analyzed data. C.-X.Z. and S.Y.H. analyzed data. Y.J.,

X.-Y.Z., C.-X.Z., and S.Y.H. wrote the paper, and all authors approved the final article.

## DECLARATION OF INTERESTS

The authors declare no competing interests.

## STAR★METHODS

Detailed methods are provided in the online version of this paper and include the following:

- [KEY RESOURCES TABLE](#)
- [EXPERIMENTAL MODEL AND SUBJECT DETAILS](#)
  - Plant materials and insects
- [METHOD DETAILS](#)
  - Transgenic rice
  - *In situ* mRNA hybridization analysis
  - Rice sheath and phloem exudate sample preparation for LC-MS
  - RNA interference (RNAi)
  - BPH survival test on artificial diet
  - BPH survival test on rice
  - pH assay
  - RNA isolation and quantitative real-time PCR (qRT-PCR)
  - Callose deposition in rice sheath
- [QUANTIFICATION AND STATISTICAL ANALYSIS](#)

## SUPPLEMENTAL INFORMATION

Supplemental information can be found online at <https://doi.org/10.1016/j.cub.2024.09.039>.

Received: October 17, 2023

Revised: August 12, 2024

Accepted: September 16, 2024

Published: October 14, 2024

## REFERENCES

- Jing, S.L., Zhao, Y., Du, B., Chen, R.Z., Zhu, L.L., and He, G.C. (2017). Genomics of interaction between the brown planthopper and rice. *Curr. Opin. Insect Sci.* **19**, 82–87. <https://doi.org/10.1016/j.cois.2017.03.005>.
- Sogawa, K. (1973). Feeding of the rice plant- and leafhoppers. *Rev. Plant Prot. Res.* **6**, 31–43.
- Ling, K.C., Tiongco, E.R., and Aguiro, V.M. (1978). Rice ragged stunt, a new virus disease. *Plant Dis. Rep.* **62**, 701–705.
- Zhou, S.X., Chen, M.T., Zhang, Y.B., Gao, Q., Noman, A., Wang, Q., Li, H., Chen, L., Zhou, P.Y., Lu, J., et al. (2019). OsMKK3, a Stress-Responsive Protein Kinase, Positively Regulates Rice Resistance to *Nilaparvata lugens* via Phytohormone Dynamics. *Int. J. Mol. Sci.* **20**, 3023–3038. <https://doi.org/10.3390/ijms20123023>.
- Du, B., Chen, R.Z., Guo, J.P., and He, G.C. (2020). Current understanding of the genomic, genetic, and molecular control of insect resistance in rice. *Mol. Breed.* **40**, 24. <https://doi.org/10.1007/s11032-020-1103-3>.
- Huang, H.J., Liu, C.W., Huang, X.H., Zhou, X., Zhuo, J.C., Zhang, C.X., and Bao, Y.Y. (2016). Screening and Functional Analyses of *Nilaparvata lugens* Salivary Proteome. *J. Proteome Res.* **15**, 1883–1896. <https://doi.org/10.1021/acs.jproteome.6b00086>.
- Rao, W., Zheng, X.H., Liu, B.F., Guo, Q., Guo, J.P., Wu, Y., Shangguan, X.X., Wang, H.Y., Wu, D., Wang, Z.Z., et al. (2019). Secretome analysis and in planta expression of salivary proteins identify candidate effectors from the brown planthopper *Nilaparvata lugens*. *Mol. Plant Microbe Interact.* **32**, 227–239. <https://doi.org/10.1094/MPMI-05-18-0122-R>.
- Liu, X.Q., Zhou, H.Y., Zhao, J., Hua, H.X., and He, Y.P. (2016). Identification of the secreted watery saliva proteins of the rice brown

- planthopper, *Nilaparvata lugens* (Stål) by transcriptome and Shotgun LC-MS/MS approach. *J. Insect Physiol.* 89, 60–69. <https://doi.org/10.1016/j.jinsphys.2016.04.002>.
9. Wang, Y.Y., Wang, X.L., Yuan, H.Y., Chen, R.Z., Zhu, L.L., He, R.F., and He, G.C. (2008). Responses of two contrasting genotypes of rice to brown planthopper. *Mol. Plant Microbe Interact.* 21, 122–132. <https://doi.org/10.1094/MPMI-21-1-0122>.
  10. Miles, P.W. (1999). Aphid saliva. *Biol. Rev.* 74, 41–85. <https://doi.org/10.1111/j.1469-185X.1999.tb00181.x>.
  11. Ji, R., Ye, W.F., Chen, H.D., Zeng, J.M., Li, H., Yu, H.X., Li, J.C., and Lou, Y.G. (2017). A Salivary Endo-beta-1,4-Glucanase Acts as an Effector That Enables the Brown Planthopper to Feed on Rice. *Plant Physiol.* 173, 1920–1932. <https://doi.org/10.1104/pp.16.01493>.
  12. Ye, W.F., Yu, H.X., Jian, Y.K., Zeng, J.M., Ji, R., Chen, H.D., and Lou, Y.G. (2017). A salivary EF-hand calcium-binding protein of the brown planthopper *Nilaparvata lugens* functions as an effector for defense responses in rice. *Sci. Rep.* 7, 40498. <https://doi.org/10.1038/srep40498>.
  13. Gong, G., Yuan, L.Y., Li, Y.F., Xiao, H.X., Li, Y.F., Zhang, Y., Wu, W.J., and Zhang, Z.F. (2022). Salivary protein 7 of the brown planthopper functions as an effector for mediating tricin metabolism in rice plants. *Sci. Rep.* 12, 3205. <https://doi.org/10.1038/s41598-022-07106-6>.
  14. Huang, H.J., Liu, C.W., Xu, H.J., Bao, Y.Y., and Zhang, C.X. (2017). Mucin-like protein, a saliva component involved in brown planthopper virulence and host adaptation. *J. Insect Physiol.* 98, 223–230. <https://doi.org/10.1016/j.jinsphys.2017.01.012>.
  15. Shangguan, X.X., Zhang, J., Liu, B.F., Zhao, Y., Wang, H.Y., Wang, Z.Z., Guo, J.P., Rao, W.W., Jing, S.L., Guan, W., et al. (2018). A Mucin-Like Protein of Planthopper Is Required for Feeding and Induces Immunity Response in Plants. *Plant Physiol.* 176, 552–565. <https://doi.org/10.1104/pp.17.00755>.
  16. Meldrum, N.U., and Roughton, F.J.W. (1933). Carbonic anhydrase. Its preparation and properties. *J. Physiol.* 80, 113–142. <https://doi.org/10.1113/jphysiol.1933.sp003077>.
  17. Engineer, C.B., Ghassemian, M., Anderson, J.C., Peck, S.C., Hu, H.H., and Schroeder, J.I. (2014). Carbonic anhydrases, EPF2 and a novel protease mediate CO<sub>2</sub> control of stomatal development. *Nature* 513, 246–250. <https://doi.org/10.1038/nature13452>.
  18. Yu, X.J., McGourty, K., Liu, M., Unsworth, K.E., and Holden, D.W. (2010). pH sensing by intracellular *Salmonella* induces effector translocation. *Science* 328, 1040–1043. <https://doi.org/10.1126/science.1189000>.
  19. Smith, K.S., and Ferry, J.G. (2000). Prokaryotic carbonic anhydrases. *FEMS Microbiol. Rev.* 24, 335–366. <https://doi.org/10.1111/j.1574-6976.2000.tb00546.x>.
  20. Henry, R.P. (1996). Multiple roles of carbonic anhydrase in cellular transport and metabolism. *Annu. Rev. Physiol.* 58, 523–538. <https://doi.org/10.1146/annurev.ph.58.030196.002515>.
  21. Zhou, Y.L., Vroegop-Vos, I.A., Van Dijken, A.J.H., Van der Does, D., Zipfel, C., Pieterse, C.M.J., and Van Wees, S.C.M. (2020). Carbonic anhydrases CA1 and CA4 function in atmospheric CO<sub>2</sub>-modulated disease resistance. *Planta* 251, 75. <https://doi.org/10.1007/s00425-020-03370-w>.
  22. Xu, H.J., Xue, J., Lu, B., Zhang, X.C., Zhuo, J.C., He, S.F., Ma, X.F., Jiang, Y.Q., Fan, H.W., Xu, J.Y., et al. (2015). Two insulin receptors determine alternative wing morphs in planthoppers. *Nature* 519, 464–467. <https://doi.org/10.1038/nature14286>.
  23. Ghaffar, M.B.A.B., Pritchard, J., and Ford-Lloyd, B. (2011). Brown planthopper (*N. lugens* Stål) feeding behaviour on rice germplasm as an indicator of resistance. *PLoS One* 6, e22137. <https://doi.org/10.1371/journal.pone.0022137>.
  24. Gjetting, K.S.K., Ytting, C.K., Schulz, A., and Fuglsang, A.T. (2012). Live imaging of intra- and extracellular pH in plants using pHusion, a novel genetically encoded biosensor. *J. Exp. Bot.* 63, 3207–3218. <https://doi.org/10.1093/jxb/ers040>.
  25. Kesten, C., Gámez-Arjona, F.M., Menna, A., Scholl, S., Dora, S., Huerta, A.I., Huang, H.Y., Tintor, N., Kinoshita, T., Rep, M., et al. (2019). Pathogen-induced pH changes regulate the growth-defense balance in plants. *EMBO J.* 38, e101822. <https://doi.org/10.15252/embj.2019101822>.
  26. Liu, L., Song, W., Huang, S., Jiang, K., Moriwaki, Y., Wang, Y., Men, Y., Zhang, D., Wen, X., Han, Z., et al. (2022). Extracellular pH sensing by plant cell-surface peptide-receptor complexes. *Cell* 185, 3341–3355.e13. <https://doi.org/10.1016/j.cell.2022.07.012>.
  27. Du, B., Zhang, W.L., Liu, B.F., Hu, J., Wei, Z., Shi, Z.Y., He, R.F., Zhu, L.L., Chen, R.Z., Han, B., et al. (2009). Identification and characterization of *Bph14*, a gene conferring resistance to brown planthopper in rice. *Proc. Natl. Acad. Sci. USA* 106, 22163–22168. <https://doi.org/10.1073/pnas.0912139106>.
  28. Guo, J.P., Xu, C.X., Wu, D., Zhao, Y., Qiu, Y.F., Wang, X.X., Ouyang, Y.D., Cai, B.D., Liu, X., Jing, S.L., et al. (2018). *Bph6* encodes an exocyst-localized protein and confers broad resistance to planthoppers in rice. *Nat. Genet.* 50, 297–306. <https://doi.org/10.1038/s41588-018-0039-6>.
  29. Wang, Y., Cao, L., Zhang, Y., Cao, C., Liu, F., Huang, F., Qiu, Y., Li, R., and Lou, X. (2015). Map-based cloning and characterization of *BPH29*, a B3 domain-containing recessive gene conferring brown planthopper resistance in rice. *J. Exp. Bot.* 66, 6035–6045. <https://doi.org/10.1093/jxb/erv318>.
  30. Hu, L., Wu, Y., Wu, D., Rao, W., Guo, J., Ma, Y., Wang, Z., Shangguan, X., Wang, H., Xu, C., et al. (2017). The coiled-coil and nucleotide binding domains of BROWN PLANTHOPPER RESISTANCE14 function in signaling and resistance against planthopper in rice. *Plant Cell* 29, 3157–3185. <https://doi.org/10.1105/tpc.17.00263>.
  31. Fu, Z.Q., and Dong, X.N. (2013). Systemic acquired resistance: turning local infection into global defense. *Annu. Rev. Plant Biol.* 64, 839–863. <https://doi.org/10.1146/annurev-arplant-042811-105606>.
  32. Innes, R. (2018). The Positives and Negatives of NPR: A Unifying Model for Salicylic Acid Signaling in Plants. *Cell* 173, 1314–1315. <https://doi.org/10.1016/j.cell.2018.05.034>.
  33. He, J., Liu, Y.Q., Yuan, D.Y., Duan, M.J., Liu, Y.L., Shen, Z.J., Yang, C.Y., Qiu, Z.Y., Liu, D.M., Wen, P.Z., et al. (2020). An R2R3 MYB transcription factor confers brown planthopper resistance by regulating the phenylalanine ammonia-lyase pathway in rice. *Proc. Natl. Acad. Sci. USA* 117, 271–277. <https://doi.org/10.1073/pnas.1902771116>.
  34. Yoshida, S.F.D., Cock, J.H., and Gomez, K.A. (1976). *Laboratory Manual for Physiological Studies of Rice, Third Edition (International Rice Research Institute)*, pp. 61–64.
  35. Hao, P.Y., Liu, C.X., Wang, Y.Y., Chen, R.Z., Tang, M., Du, B., Zhu, L.L., and He, G.C. (2008). Herbivore-induced callose deposition on the sieve plates of rice: an important mechanism for host resistance. *Plant Physiol.* 146, 1810–1820. <https://doi.org/10.1104/pp.107.111484>.
  36. Guo, J., Wang, H., Guan, W., Guo, Q., Wang, J., Yang, J., Peng, Y., Shan, J., Gao, M., Shi, S., et al. (2023). A tripartite rheostat controls self-regulated host plant resistance to insects. *Nature* 618, 799–807. <https://doi.org/10.1038/s41586-023-06197-z>.
  37. Huang, H.J., Wang, Y.Z., Li, L.L., Lu, H.B., Lu, J.B., Wang, X., Ye, Z.X., Zhang, Z.L., He, Y.J., Lu, G., et al. (2023). Planthopper salivary sheath protein LsSP1 contributes to manipulation of rice plant defenses. *Nat. Commun.* 14, 737. <https://doi.org/10.1038/s41467-023-36403-5>.
  38. Huang, H.J., Cui, J.R., Xia, X., Chen, J., Ye, Y.X., Zhang, C.X., and Hong, X.Y. (2019). Salivary DNase II from *Laodelphax striatellus* acts as an effector that suppresses plant defence. *New Phytol.* 224, 860–874. <https://doi.org/10.1111/nph.15792>.
  39. Elzinga, D.A., De Vos, M., and Jander, G. (2014). Suppression of plant defenses by a *Myzus persicae* (green peach aphid) salivary effector protein. *Mol. Plant Microbe Interact.* 27, 747–756. <https://doi.org/10.1094/MPMI-01-14-0018-R>.
  40. Su, Q., Peng, Z., Tong, H., Xie, W., Wang, S., Wu, Q., Zhang, J., Li, C., and Zhang, Y. (2019). A salivary ferritin in the whitefly suppresses plant defenses and facilitates host exploitation. *J. Exp. Bot.* 70, 3343–3355. <https://doi.org/10.1093/jxb/erz152>.

41. Fu, J., Shi, Y., Wang, L., Zhang, H., Li, J., Fang, J., and Ji, R. (2020). Planthopper-Secreted Salivary Disulfide Isomerase Activates Immune Responses in Plants. *Front. Plant Sci.* *11*, 622513. <https://doi.org/10.3389/fpls.2020.622513>.
42. Murphy, E., and De Smet, I. (2014). Understanding the RALF family: a tale of many species. *Trends Plant Sci.* *19*, 664–671. <https://doi.org/10.1016/j.tplants.2014.06.005>.
43. Abarca, A., Franck, C.M., and Zipfel, C. (2021). Family-wide evaluation of RAPID ALKALINIZATION FACTOR peptides. *Plant Physiol.* *187*, 996–1010. <https://doi.org/10.1093/plphys/kiab308>.
44. Haruta, M., Sabat, G., Stecker, K., Minkoff, B.B., and Sussman, M.R. (2014). A peptide hormone and its receptor protein kinase regulate plant cell expansion. *Science* *343*, 408–411. <https://doi.org/10.1126/science.1244454>.
45. Koh, E.J., Zhou, L., Williams, D.S., Park, J., Ding, N., Duan, Y.P., and Kang, B.H. (2012). Callose deposition in the phloem plasmodesmata and inhibition of phloem transport in citrus leaves infected with “*Candidatus Liberibacter asiaticus*”. *Protoplasma* *249*, 687–697. <https://doi.org/10.1007/s00709-011-0312-3>.
46. Ernst, A.M., Jekat, S.B., Zielonka, S., Müller, B., Neumann, U., Rüping, B., Twyman, R.M., Krzyzaneck, V., Prüfer, D., and Noll, G.A. (2012). Sieve element occlusion (SEO) genes encode structural phloem proteins involved in wound sealing of the phloem. *Proc. Natl. Acad. Sci. USA* *109*, E1980–E1989. <https://doi.org/10.1073/pnas.1202999109>.
47. Batailler, B., Lemaître, T., Vilaine, F., Sanchez, C., Renard, D., Cayla, T., Beneteau, J., and Dinant, S. (2012). Soluble and filamentous proteins in Arabidopsis sieve elements. *Plant Cell Environ.* *35*, 1258–1273. <https://doi.org/10.1111/j.1365-3040.2012.02487.x>.
48. Jiang, Y.J., Zhang, C.X., Chen, R.Z., and He, S.Y. (2019). Challenging battles of plants with phloem-feeding insects and prokaryotic pathogens. *Proc. Natl. Acad. Sci. USA* *116*, 23390–23397. <https://doi.org/10.1073/pnas.1915396116>.
49. Hattori, M., Komatsu, S., Noda, H., and Matsumoto, Y. (2015). Proteome Analysis of Watery Saliva Secreted by Green Rice Leafhopper, *Nephotettix cincticeps*. *PLoS One* *10*, e0123671. <https://doi.org/10.1371/journal.pone.0123671>.
50. Guo, H., Zhang, Y., Li, B., Li, C., Shi, Q., Zhu-Salzman, K., Ge, F., and Sun, Y. (2023). Salivary carbonic anhydrase II in winged aphid morph facilitates plant infection by viruses. *Proc. Natl. Acad. Sci. USA* *120*, e2222040120. <https://doi.org/10.1073/pnas.2222040120>.
51. Yang, Y.L., and Sourjik, V. (2012). Opposite responses by different chemoreceptors set a tunable preference point in *Escherichia coli* pH taxis. *Mol. Microbiol.* *86*, 1482–1489. <https://doi.org/10.1111/mmi.12070>.
52. Hayashi, M., Fukuzawa, T., Sorimachi, H., and Maeda, T. (2005). Constitutive activation of the pH-responsive Rim101 pathway in yeast mutants defective in late steps of the MVB/ESCRT pathway. *Mol. Cell. Biol.* *25*, 9478–9490. <https://doi.org/10.1128/MCB.25.21.9478-9490.2005>.
53. Shen, J., Zeng, Y.L., Zhuang, X.H., Sun, L., Yao, X.Q., Pimpl, P., and Jiang, L.W. (2013). Organelle pH in the Arabidopsis Endomembrane System. *Mol. Plant* *6*, 1419–1437. <https://doi.org/10.1093/mp/sst079>.
54. Schneider, C.A., Rasband, W.S., and Eliceiri, K.W. (2012). NIH Image to ImageJ: 25 years of image analysis. *Nature Methods* *9*, 671–675. <https://doi.org/10.1038/nmeth.2089>. <https://pubmed.ncbi.nlm.nih.gov/22930834/>.
55. Gaupels, F., Knauer, T., and van Bel, A.J.E. (2008). A combinatory approach for analysis of protein sets in barley sieve-tube samples using EDTA-facilitated exudation and aphid stylectomy. *J. Plant Physiol.* *165*, 95–103. <https://doi.org/10.1016/j.jplph.2007.07.023>.
56. Du, B., Wei, Z., Wang, Z., Wang, X., Peng, X., Du, B., Chen, R., Zhu, L., and He, G. (2015). Phloem-exudate proteome analysis of response to insect brown plant-hopper in rice. *J. Plant Physiol.* *183*, 13–22. <https://doi.org/10.1016/j.jplph.2015.03.020>.

STAR★METHODS

KEY RESOURCES TABLE

REAGENT or RESOURCE	SOURCE	IDENTIFIER
<b>Antibodies</b>		
Rabbit polyclonal anti-HA	Zenbio	Cat#301113; RRID: AB_3662580
Mouse monoclonal anti-GFP	Abmart	Cat#M20004; RRID: AB_2619674
<b>Bacterial strains</b>		
<i>Escherichia coli</i> DH5a	TransGen	CD201-01
<i>Agrobacterium tumefaciens</i> GV3101	N/A	N/A
<b>Chemicals</b>		
Phusion High-Fidelity DNA Polymerase	Thermo Scientific	Cat#F534
Gateway LR Clonase II Enzyme mix	Invitrogen	Cat#11791100
Gateway BP Clonase II Enzyme mix	Invitrogen	Cat#11789020
ProtoScript II Reverse Transcriptase	NEB	Cat#M0368
SYBR Green Mix	Roche	Cat#4887352001
<b>Oligonucleotides</b>		
NICA-overlap-F; NICA-overlap-R	ggggacaagttgtacaataaacgaggcttc ATGGAGCTTTTCTCCACATA; ggggaccactttgtacaagaagctgggtc CTAACAGTATCTGTGATTTGATTGTATC	Sangon Biotech
NICA-overlap-1-F; NICA-overlap-1-R	AACATTGCCTGTGCCTGGGGC AGAAATGATATAATGGGCAGC; CCCCAGGCACAGGCAATGTTG TCATAAATATAGCGATTTGACAG	Sangon Biotech
NICA-overlap-2-F; NICA-overlap-2-R	CGATGGCATGCGCCATGGTAAC TTTTAATGAAAATACGGAACC; TACCATGGCGCATGCCATCGGA TAGGATTCTGCATCGATG	Sangon Biotech
NICA-overlap-3-F; NICA-overlap-3-R	TGGGCAGCGCTCACTTCATCGA TGCAGAATCGTATCCGAT; GATGAAGTGAGCGCTGCCCAT TATATCATTCTGCCCCAGT	Sangon Biotech
NICA-overlap-4-F; NICA-overlap-4-R	CAGTCACGGCCATCATTCTGCC AATTGCTGTTGGTATATCC; CAGAATGATGGCCGTGACTGG CTTCTGTAAGGGTGGCGT	Sangon Biotech
NICA-overlap-5-F; NICA-overlap-5-R	CCAGTTCTCTAGCAACGCCAC CCTTTACAGAAGCAGTCACG; GGCGTTGCTAGAGAACCTGGA TAAGCAAAGTATTCTGGTTTATG	Sangon Biotech
NICA-qRT-F; NICA-qRT-R	CCTTGCTGCGTACATTGA; CGGTTCTGTGATTGAGTGT	Sangon Biotech
NI18S rRNA-qRT-F; NI18S rRNA-qRT-R	CGCTACTACCGATTGAA; GGAAACCTTGTTACGACTT	Sangon Biotech
OsACTIN-qRT -F; OsACTIN-qRT -R	TGGACAGGTTATCACCATTGGT; CCGCAGCTTCCATTCCATG	Sangon Biotech
OsWRKY45-qRT -F; OsWRKY45-qRT -R	GGGAATTCGGTGGTCGTCAA; TGGATCTCCTTCTGCCCGTA	Sangon Biotech
OsPBZ1-qRT -F; OsPBZ1-qRT -R	GGGTGTGGGAAGCACATACA; CCTCGAGCACATCCGACTTT	Sangon Biotech
OsNH1-qRT -F; OsNH1-qRT -R	TGGCAGGTGAGAGTCTACGA; GCTACTCTTGCCCTCCATCGG	Sangon Biotech

(Continued on next page)

**Continued**

REAGENT or RESOURCE	SOURCE	IDENTIFIER
OsNH2-qRT -F; OsNH2-qRT -R	GTGGATACACGGCACTCCAT; CTCTGGCCATCAGCAGTCAA	Sangon Biotech
OsWRKY13-F; OsWRKY13-R	CAGTAGCTCCAAGGGGTGTC; CGAAGGAGTAGGTGACGAGC	Sangon Biotech
<b>Software</b>		
ImageJ	Schneider et al. <sup>54</sup>	<a href="https://imagej.nih.gov/ij/">https://imagej.nih.gov/ij/</a>
GraphPad Prism version 8	San Diego, California USA	<a href="https://www.graphpad.com">https://www.graphpad.com</a>

**EXPERIMENTAL MODEL AND SUBJECT DETAILS**

**Plant materials and insects**

*Oryza sativa* ssp. *Japonica* cv. Nipponbare was used as the wild type and for generating transgenic plants. The *Nilaparvata lugens* population used in this study was originally derived from a rice field on the Huajiachi Campus of Zhejiang University, Hangzhou (30° 16' N, 120° 11' E), China, in 2008, and artificially propagated for many generations until now. BPH insects were reared in environmentally controlled growth chambers on a susceptible cultivar rice variety Xiushui 134 at 27 ± 0.5°C and 50 ± 0.5% relative humidity under a 16-h light and 8-h dark photoperiod in a modified Yoshida solution (in which ammonium nitrate was replaced by 1.06 M carbamide) with pH of 4.

**METHOD DETAILS**

**Transgenic rice**

The *NICA* coding sequence was amplified from BPH. Several *NICA* mutants (*NICA-m1*, *NICA-m2*, and *NICA-m3*) were made by site-directed mutagenesis. The *NICA-m1*, *NICA-m2* and *NICA-m3* PCR products encoding proteins in which His<sup>159</sup> and His<sup>161</sup> were mutated to Ala, Glu<sup>182</sup> and His<sup>184</sup> were replaced by Ala, and all seven conserved active site residues, His<sup>159</sup>, His<sup>161</sup>, Glu<sup>171</sup>, Glu<sup>182</sup>, His<sup>184</sup>, Thr<sup>269</sup> and Phe<sup>279</sup>, were changed to Ala, respectively. The WT and mutant *NICA* PCR products were recombined into the intermediate vector pDonor207 using the BP recombination kit (Invitrogen), and then recombined into the destination vector pEarleygate104 using the LR recombination kit (Invitrogen) to generate P<sub>35S</sub>::*NICA-YFP* and P<sub>35S</sub>::mutant *NICA-YFP* expression vectors. The transgenic rice plants were generated by Agrobacterium-mediated transformation at BIOGLE GeneTech (Hangzhou Biogle Co., LTD.) where rice plants were reared in a greenhouse at 27 ± 0.5°C and 60 ± 0.5% relative humidity under a 16-h light and 8-h dark photoperiod.

**In situ mRNA hybridization analysis**

Fresh salivary tissues were isolated from 100 5<sup>th</sup> instar BPH and washed 3 times before being placed in the 4% paraformaldehyde (PFA) fix solution (Servicebio, G1113) at 4°C overnight, dehydrated and embedded in paraffin. Ten μM-thick sections were cut on glass slides, dewaxed and digested by Protease K (Servicebio, G1205) at 37°C for 15 min. After three washes in phosphate buffered saline (PBS) buffer (Servicebio, G0020), the sections were incubated in pre-hybridization solution at 37°C for 1 h and then in hybridization solution containing the *NICA* probe (1 μM) at 42°C overnight. The PCR primer for generating the probe was 5'-GGTTCTGTGATTGAGTGTTGGATCTCCCTGCG-3' with a single-end CY3 tag generated using the DIG RNA Labeling Kit (Roche Applied Science, Penzberg, Germany) based on the manufacturer's instructions. The slides were stained with DAPI for 8 min in the dark after being washed in saline sodium citrate (SSC) buffer (Servicebio, G3016-4) for three times (2 × SSC, 10 min; 1 × SSC, 2 × 5 min; 0.5 × SSC, 10 min). Sections hybridized with sense probe was used as a negative control and antisense probe was used to detect the target mRNA. All steps were performed at 37°C and sections were examined under a Nikon fluorescence microscope with a 40 × lens (330 nm–380 nm for DAPI, 510 nm–560 nm for CY3).

**Rice sheath and phloem exudate sample preparation for LC-MS**

Three independent sets of Nipponbare rice sheath protein samples (three biological replicates) were collected after feeding by 5<sup>th</sup> instar nymphs as follows. Briefly, ten 6-leaf-stage rice plants were individually placed into a breathable transparent plastic bottle (5 cm in diameter, 30 cm in height) containing Yoshida medium, pH = 4, and then fed by ~500 fifth instar BPH for 72 h. Next, BPHs were gently shaken off leaves with intact stylets and the two outermost layers of leaf sheath surrounding the stem were cut into small pieces, rinsed with ultrapure water for three times and ground to powder in liquid nitrogen. Total protein was extracted in a buffer containing 60 mM Tris-HCl (pH = 7.6), 2.5% Glycerol, 6% SDS, 0.1 M DL-Dithiothreitol (DTT), 1x Protein inhibitor cocktail and 1 mM phenylmethanesulfonyl fluoride. Protein samples were concentrated using 3-kDa filtration units and shipped on dry ice to Shanghai Hoogen Biotech for shot-gun LC-MS analysis. Briefly, protein samples digested by trypsin for 16 h at 37°C. The hydrolysates were then loaded into Zorbax 300SB-C18 peptide traps (Agilent Technologies, Wilmington, DE) and analyzed by a Q Exactive

mass spectrometer (Thermo Fisher). The raw LC-MS data were searched against the BPH protein database (NCBI Accession No. PRJNA669454) using software MaxQuant 1.5.5.1. Peptides with a high confidence score was extracted, and the database search was conducted with false discovery rate (FDR) under 0.01.

For phloem exudate collection, 4-leaf-stage rice plants were used. Exudates were collected using the EDTA-facilitated exudation method as described by Gaupels et al.<sup>55</sup> and Du et al.<sup>56</sup> with some modifications. Briefly, the shoots of plants were cut just above the stem/root junction with a sharp razor blade while rootless shoots were submerged in a 20 mM EDTA solution (pH 8.0, established using KOH), and shaken for 15 seconds to remove compounds from damaged roots. Then 4–6 rootless plants were transferred to plastic tubes containing 1.5 mL fresh 20 mM EDTA solution (pH 8.0) to facilitate phloem sap exudation. Plants were placed in a dark, high humid chamber to reduce transpiration. The exudates were collected after 12 h and the samples were concentrated by centrifugation at 4°C in a 2 mL concentrator (10 kDa for NICA concentration; 30 kDa for NICA-YFP concentration) to a final volume of 20  $\mu$ L (from a total of 40 plants) for Western blot or LC-MS analysis.

### RNA interference (RNAi)

The nucleotide sequence (around 500 bp long) specific to the *NICA* coding region was cloned into the pMD 19-T vector (TAKARA). The double-stranded RNA was synthesized through PCR amplification by using the Mega script T7 High Yield RNA Transcription Kit (Vazyme, Nanjing, China), following the manufacturer's instructions. The procedure for gene knockdown by RNAi was described previously.<sup>22</sup> Briefly, the 2<sup>nd</sup> and 5<sup>th</sup> instar BPH nymphs in an insect rearing growth chamber were anaesthetized with carbon dioxide for  $\sim$ 10 s. Approximately 50–250 ng of dsRNA was injected into BPH mesothorax using FemtoJet (Eppendorf-Netheler-Hinz, Hamburg, Germany). The efficiency of RNA interference was assessed 48 h after injection. RNA from 30 nymphs was extracted using the RNAiso Plus kit (TaKaRa) according to the manufacturer's instructions as one biological replicate. The relative level of the *NICA* transcript was quantified using a CFX96TM Real-Time PCR Detection System (Bio-Rad, Hercules, CA, USA) with primers shown in [key resources table](#). The *Aequorea Victoria* green fluorescent protein (GFP) gene sequence was used as the control template in RNAi experiments. Four biological replicates (30 individual insects pooled for each biological replicate) were conducted.

### BPH survival test on artificial diet

The 5<sup>th</sup> instar BPH nymphs injected with *dsGFP* or *dsNICA* were immediately placed on one-week-old rice seedlings (1-leaf-stage) for recovery in the small breathable transparent plastic bottle for 3 days. Fifty normal-appearing BPH adults were gently transferred into a shaded black plastic bottle of 5 cm in diameter and 15 cm in height, with translucent double-layer parafilm loaded with fresh artificial diet. The first layer of parafilm closed to BPH was needled 40 holes by a 1 ml syringe and fresh artificial diet AADM, pH of 6.0, was filtered through a 0.22 micrometer needle-type bacterial filter (Sangon Biotech, F513142-0001). Fresh artificial diet was replaced every 24 hours. The second layer of parafilm wrapped the artificial diet to isolate the diet from bacteria in the air. Dead BPHs were separated from live BPHs daily and mucus adhering to the inner wall of the black plastic bottle was cleaned daily to eliminate possible impact on live BPHs. and the pH was changed from 6.8 to 6. There were three biological replicates for each treatment, and each biological replicate includes 50 BPH adults. Experiments were repeated three times with similar trends.

### BPH survival test on rice

BPH nymphs with verified *NICA* knockdown by RNAi were placed into a small breathable transparent plastic bottle of 10 cm in diameter and 9 cm in height containing one-week-old rice seedlings (1-leaf-stage) for 12 h to recover. About 20 healthy-appearing 2<sup>nd</sup> instar nymphs were gently transferred into a longer breathable transparent plastic bottle of 5 cm in diameter and 30 cm in height containing four-week-old rice plants (4- to 5-leaf-stage) and observed for up to 15 days. The feeding space for BPH in each plastic bottle was around 200 cm<sup>3</sup> divided by two sponges of 5 cm in diameter and 2 cm in thickness. The number of surviving BPHs were counted daily on each plant. *dsGFP* BPH were used as control. The average of survival rate on each seedling was calculated.

For BPH survival test on normal and acidic media growing rice plants, the early 5<sup>th</sup> instar BPH nymphs inoculated *dsGFP* and *dsNICA* fed on one-week-old rice seedlings (1-leaf-stage) were recovered in the small breathable transparent plastic bottle for 24 hours. The Nipponbare rice plants (5-leaf stage) growing on normal liquid media (pH = 4) was transferred into fresh liquid media with pH of 4 and 2 for 24 hours, respectively, before conducting BPH survival test. There were five biological replicates for every treatment, and one biological replicate is one rice plant fed by 20 BPHs. Experiments were repeated three times with similar trends.

### pH assay

Transgenic rice plants expressing the cyto-pHusion pH sensor were grown in the modified Yoshida medium as described above. Each 5-leaf-stage seedlings were fed by 30 5<sup>th</sup> instar BPH, which were starved in the breathable plastic tubes for 3 h before feeding. No BPH treatment was included as control. The microscopic images were taken from rice leaf sheaths that were fed by BPH for 1.5 h, 4 h, 8h and 12 h using an Olympus FV3000 with a 40.0 x objective. EGFP was imaged with  $\lambda_{Em}$  = 540 nm and the detection wavelength at 500–540 nm. mRFP was imaged with  $\lambda_{Em}$  = 570 nm and detection wavelength was 570 to 620 nm. Mean fluorescent intensities of EGFP and mRFP from multiple images were quantified using Fiji Image J. Briefly, the EGFP and mRFP merged images were separated into the EGFP channel and the mRFP channel with a threshold of 1–4090 using Image J. Mean intensities of EGFP and mRFP fluorescence in a region of interest (ROI) were measured to calculate the EGFP: mRFP ratio. Each treatment includes > 24 circular areas of leaf sheath with a diameter of 100  $\mu$ m each, including the feeding site at the center.

### RNA isolation and quantitative real-time PCR (qRT-PCR)

The total RNA was extracted using the TRIzol reagent kit (Invitrogen), and then treated with Rnase-free Dnase I (Invitrogen) according to the manufacturer's protocol. The RNA was reverse-transcribed using a cDNA synthesis kit (TaKaRa) and one  $\mu\text{g}$  of each RNA sample was reverse transcribed. qRT-PCR was performed from cDNA using SYBR Green qPCR mix (TaKaRa, RR601A) following the manufacturer's instructions using the LightCycler 480 system (Roche Diagnostics). Fold changes were calculated using the  $\Delta\text{Ct}$  method. Each assay was replicated at least three times, each with three biological replicates (independent RNA preparations). The rice Actin gene (*LOC\_Os03g50885*) and the BPH 18S rRNA (*LOC\_111047943*) gene were used as a reference. Sequences of qRT-PCR primers are given in [key resources table](#).

### Callose deposition in rice sheath

For counting callose deposition, four-leaf-stage rice plants were infested with  $\sim 15$  fifth instar BPH. The two outermost rice leaf sheaths were collected before and after BPH feeding for 72 h and fixed in FAA solution as described by Guo et al.,<sup>28</sup> dehydrated and embedded in paraffin. The sections were cut to 5  $\mu\text{m}$  thickness on glass slides, dewaxed and stained with 0.1 % aniline blue in 0.1 % 5 M  $\text{K}_2\text{PHO}_4$  for 10 min, and examined under Zeiss confocal microscope with a 40 $\times$  oil objective lens. The total area and number of callose deposition in the rice sieve pores were counted. Each treatment has at least 400 cross sections and 12 biological replicates.

### QUANTIFICATION AND STATISTICAL ANALYSIS

All statistics were performed using GraphPad Prism version 8 for Windows, GraphPad Software, San Diego, California USA, <https://www.graphpad.com>. Statistical details relating to specific experiments can be found in relevant Figure legends. In all cases pair-wise comparisons were performed using Student's t-test, comparisons across multiple groups were performed using ANOVA with Tukey's HSD test for significance.



**Current Biology, Volume 34**

**Supplemental Information**

**Rapid intracellular acidification  
is a plant defense response  
countered by the brown planthopper**

**Yanjuan Jiang, Xiao-Ya Zhang, Shaoqin Li, Yu-Cheng Xie, Xu-Mei Luo, Yongping Yang, Zhengyan Pu, Li Zhang, Jia-Bao Lu, Hai-Jian Huang, Chuan-Xi Zhang, and Sheng Yang He**

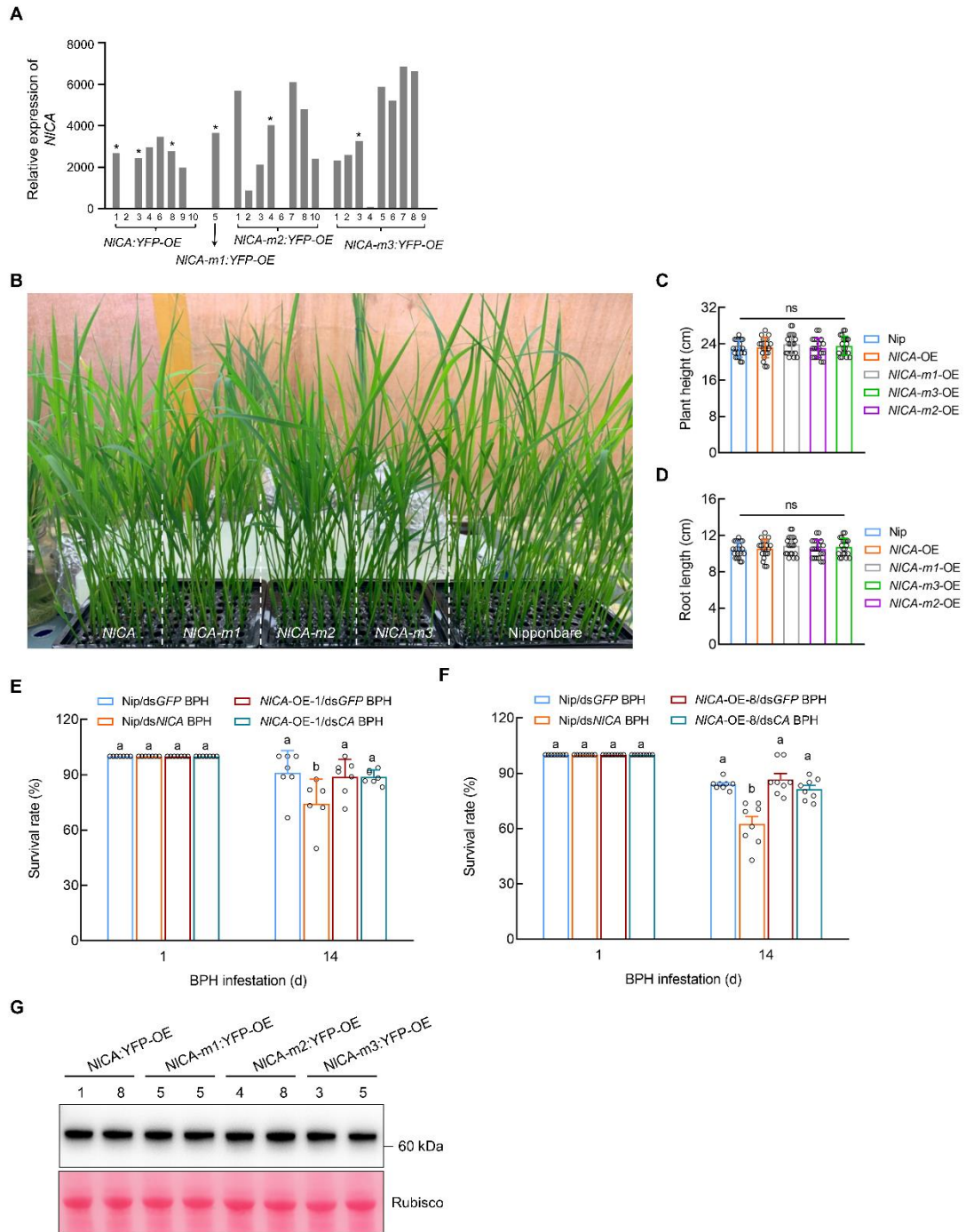


**Figure S1. Generation of *NICA*-OE and mutant *NICA*-OE plants and survival rates of BPH, related to Figure 2.** (A) qRT-PCR analysis of the *NICA* transcript levels in *NICA*-OE, *NICA*-*m1*-OE, *NICA*-*m2*-OE *NICA*-*m3*-OE plants. Plant lines labeled with an asterisk were selected for further BPH feeding assay. (B) 21-day-old of Nipponbare, *NICA*-OE, *NICA*-*m1*-OE, *NICA*-*m2*-OE *NICA*-*m3*-OE plants grown in the modified Yoshida medium. *NICA*-OE, *NICA*-*m1*-OE, *NICA*-*m2*-OE *NICA*-*m3*-OE plants displayed normal appearance compared with Nipponbare. (C and D) Plant height (C) and root length (D), respectively, in (B). Values are displayed as mean  $\pm$  SD ( $n = 20$  plants). ns indicate no significant statistically differences analyzed by one-way ANOVA (Tukey test). (E and F) The survival rates of ds*GFP* and ds*NICA* BPH insects on

Nipponbare and *NICA* transgenic plant line 3 (E) and line 8 (F) after 1-day and 14-days post-infestation. Values are displayed as mean  $\pm$  SEM (n = 8 biological replicates; 20 individual insects per each biological replicate). (G) Protein samples were extracted from one-week-old seedlings of *NICA*-OE (lines 1 and 8) and *NICA*-mutant-OE (line 5 of *NICA*-m1, lines 4 and 8 of *NICA*-m2 and lines 3 and 5 of *NICA*-m3) plants. Abundance of fusion proteins were detected with anti-GFP (Abmart, 20004). Ponceau S staining of Rubisco confirmed equal loading. Experiments were repeated three times with similar trends.

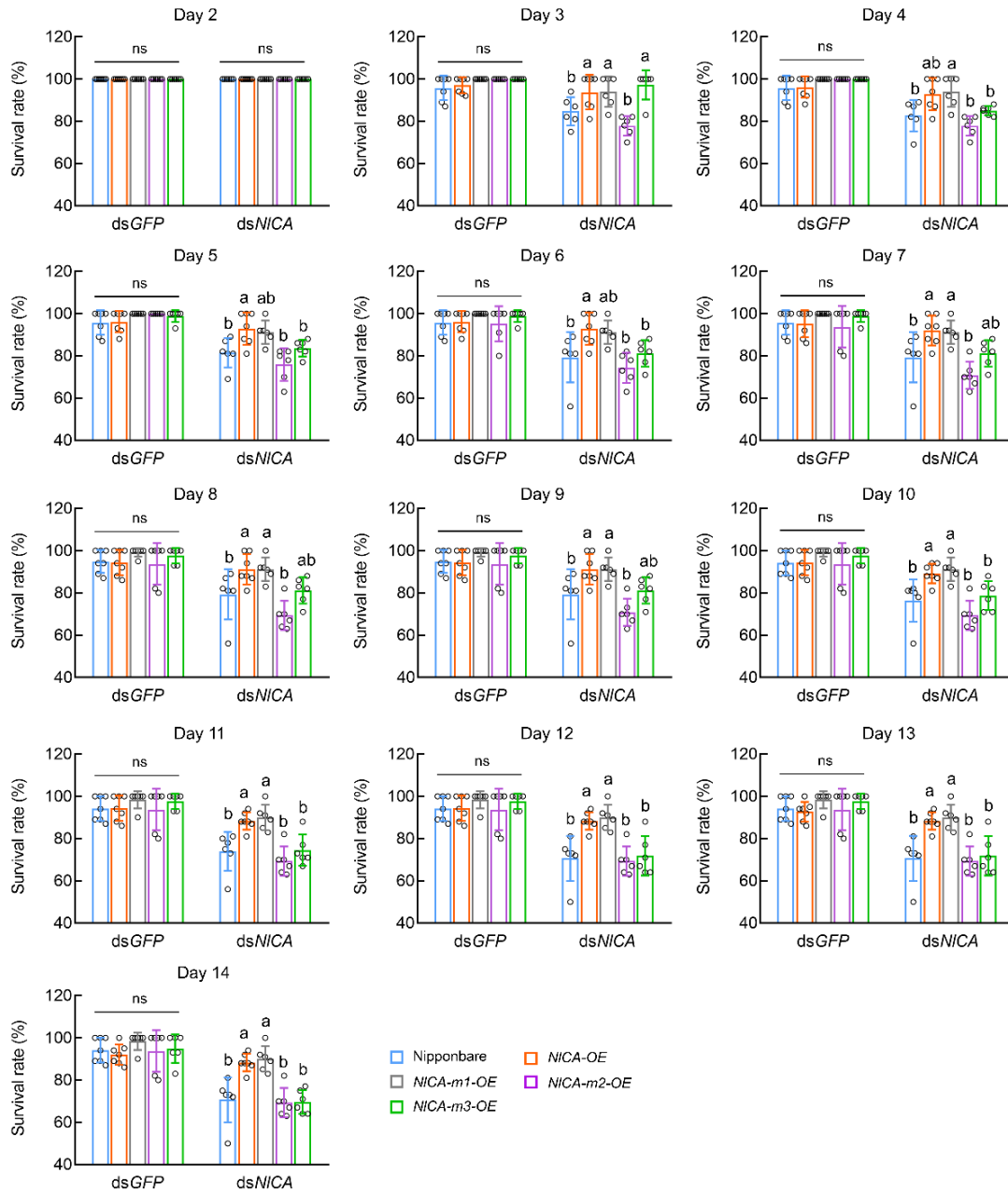


**Figure S2. The daily survival rates of dsGFP and dsNICA BPH insects on Nipponbare and NICA transgenic plants., related to Figure 2.** Values are represented as mean  $\pm$  SEM ( $n > 6$  biological replicates; 20 individual insects per each biological replicate). Different letters indicate statistically significant differences analyzed by two-way ANOVA (Tukey test,  $P < 0.05$ ). Experiments were repeated three times with similar trends.

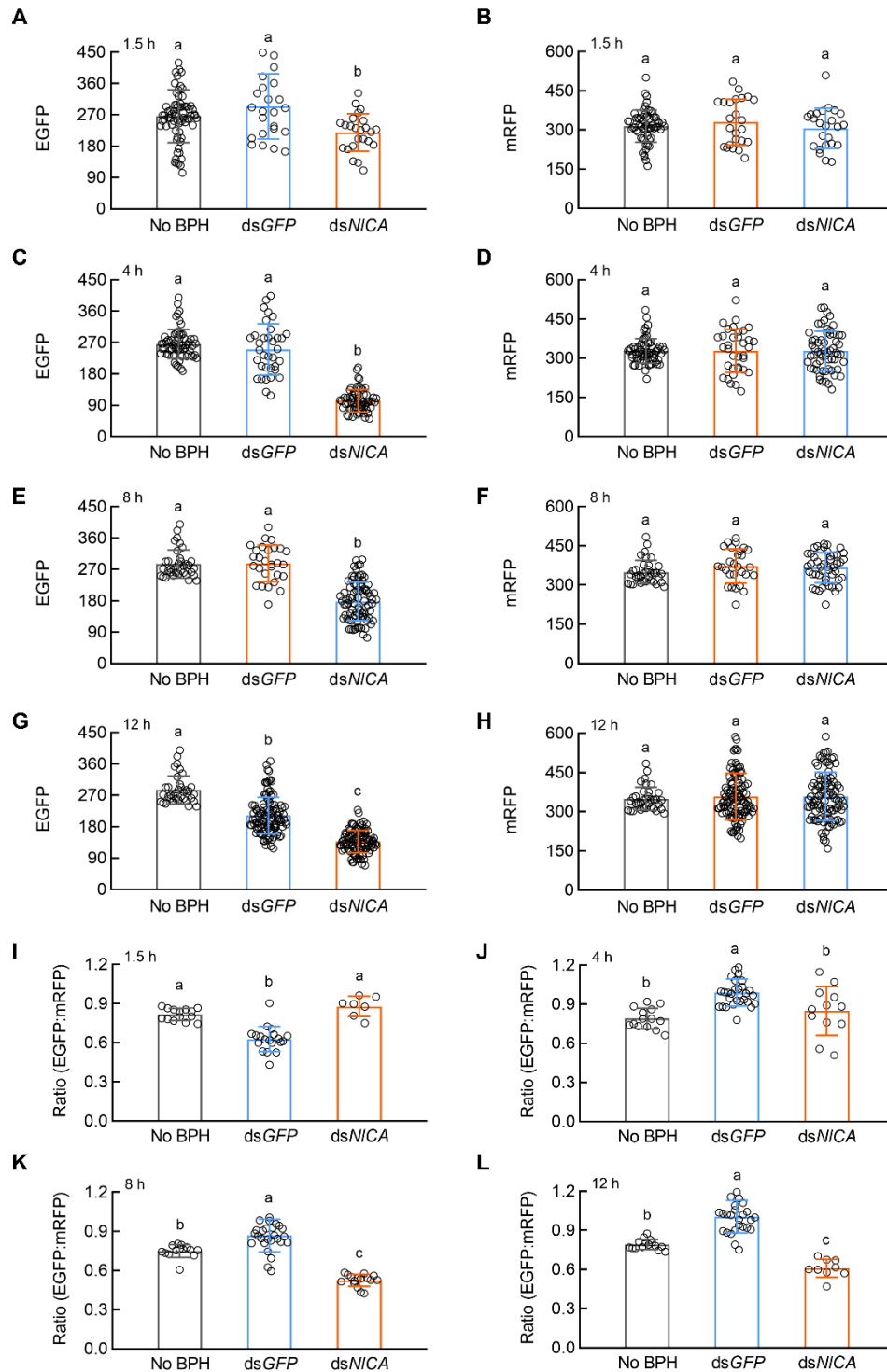


**Figure S3. Quantification of fluorescent signals in leaf sheaths of Nipponbare plants expressing the cyto-pHusion ratiometric pH sensor in response to BPH feeding, related to Figure 3.** (A, C, E, G) eGFP fluorescence intensity at 1.5, 4, 8 and 12 h after BPH feeding. (B, D, F, H) mRFP fluorescence intensity at 1.5, 4, 8 and 12 h after BPH feeding. Values are displayed as mean  $\pm$  SEM ( $n > 14$  feeding sites for each genotype). (I–L) Intracellular acidification of the mesophyll cells and epidermal cells at BPH feeding sites. EGFP:mRFP signal ratios at 1.5 h (I), 4 h (J), 8 h (K) and 12 h (L) of dsGFP or dsNICA BPH feeding compared with no BPH control. EGFP was imaged at  $\lambda_{Ex} = 500$  nm and  $\lambda_{Em} = 540$  nm. mRFP was imaged at  $\lambda_{Ex} = 570$  nm and  $\lambda_{Em} = 620$  nm. Values are displayed as mean  $\pm$  SEM ( $n \geq 16$  circular areas of leaf sheath, each circular area had a diameter of 100  $\mu$ m with the feeding site at the center).

Image processing and analysis was performed by Fiji. Different letters indicate statistically significant differences analyzed by one-way ANOVA (Tukey test,  $P < 0.05$ ).

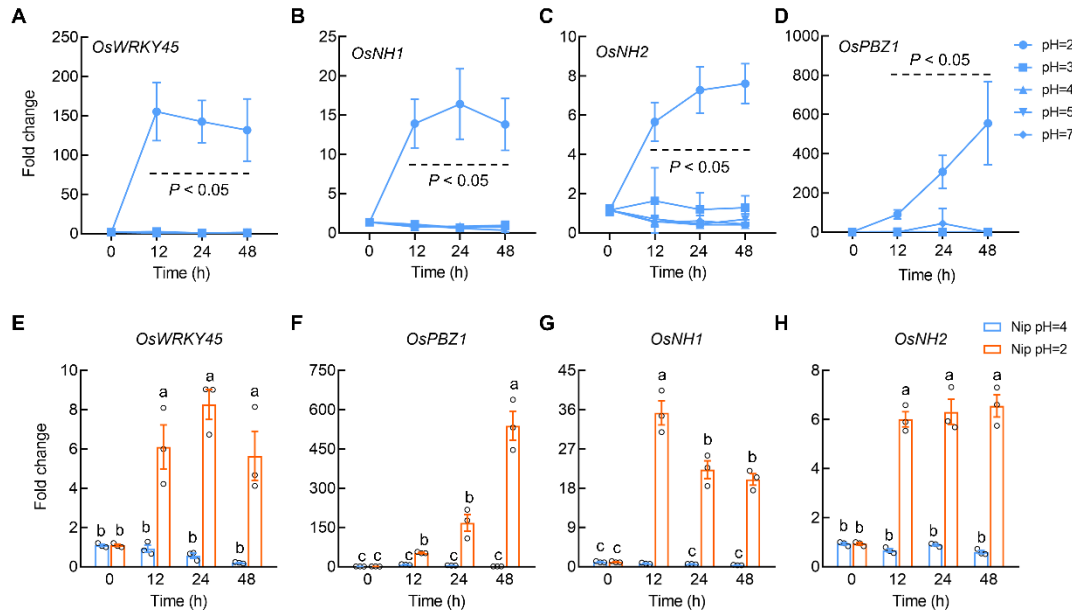


**Figure S4. Defense response genes are modulated by ectopic pH manipulation in rice, related to Figure 3.** (A-D) Expression levels of defense response genes, *OsWRKY45* (A), *OsNH1* (B), *OsNH2* (C) and *OsPBZ1* (D), are induced after acidification of Yoshida medium in which WT Nipponbare plants were grown. Rice plants were first grown in Yoshida media with pH of 4 to 5-leaf-stage and were then placed into fresh Yoshida medium with different pH for 48 h. RNA samples collected from the stem tissues for RT-qPCR in the indicated time. (E-H) Expression levels of defense response genes, *OsWRKY45* (E), *OsPBZ1* (F), *OsNH1* (G) and *OsNH2* (H), are induced after acidification of Yoshida medium in which WT Nipponbare plants were grown. Rice plants were first grown in Yoshida media with pH of 4 to 5-leaf-stage and were then placed into fresh Yoshida medium with pH of 4 or pH of 2 for 48 h. RNA samples collected from the stem tissues for RT-qPCR in the indicated time. Values represent mean  $\pm$  SEM (Two-way ANOVA,  $n = 4$ ). Different letters indicate statistically significant differences analyzed by two-way ANOVA (Tukey test,  $P < 0.05$ ). Experiments were repeated three times with similar trends.

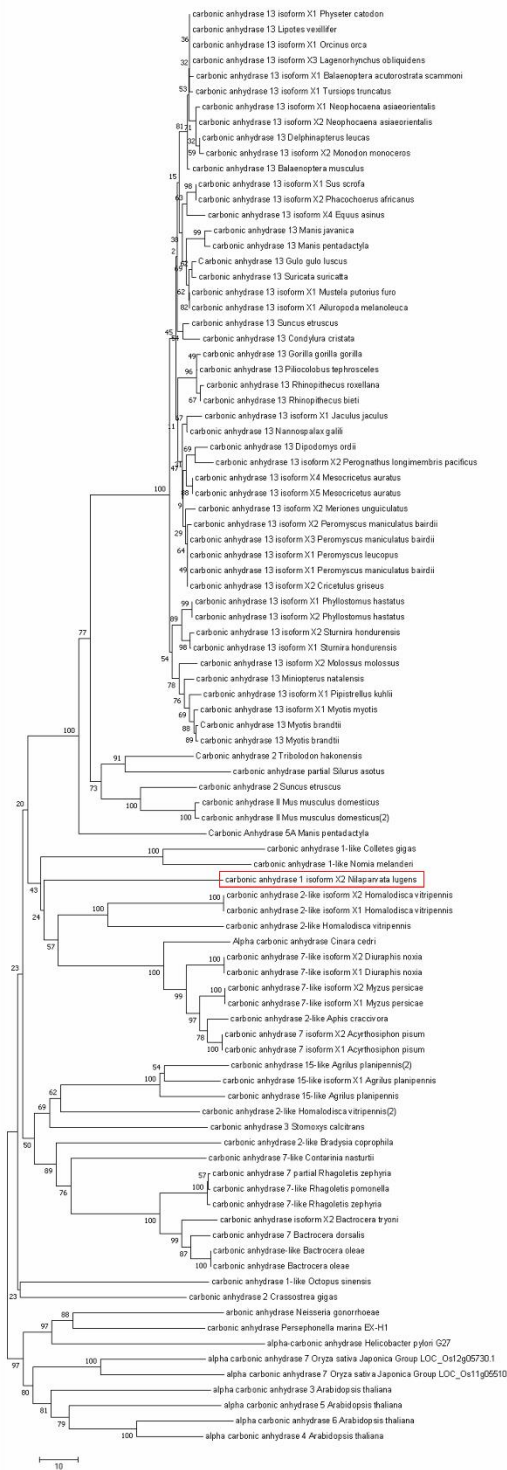


**Figure S5. Phylogenetic analysis of carbonic anhydrase proteins from representative bacteria, insect, mammal, and plant species, related to Figure 1.** The protein sequences were obtained from NCBI ([www.ncbi.nlm.nih.gov](http://www.ncbi.nlm.nih.gov)), TAIR (<http://www.arabidopsis.org/>) and Rice Genome Annotation Project (<http://rice.uga.edu/index.shtml>). Red rectangle denotes NICA. Sequence alignment was performed using Clustal W, and the phylogenetic tree was generated by MEGA 7.0 using the Neighbor–Joining method. Bootstrap values from 1,000 replicates were used to assess the robustness of the tree. The scale indicates the average number of substitutions per site.



Gene ID	Description	Accession number	References
chr11.0266.t1	<i>Nilaparvata lugens</i> uncharacterized protein (LOC11106027)	XM_022347943.1	This study
chr06.1357.t1	<i>Nilaparvata lugens</i> serpin B5 (LOC111051915)	XM_022338506.1	This study
chr07.0208.t1	<i>Nilaparvata lugens</i> 46 kDa FK506-binding nuclear protein (LOC111043757)	XM_022328800.1	This study
chr05.0798.t1	<i>Nilaparvata lugens</i> carbonic anhydrase 1-like isoform X3, NICA	XP_022198625.1	S1
chr02.2197.t1	<i>Nilaparvata lugens</i> peritrophin-like protein	KU365934.1	S1
chr03.1919.t2	<i>Nilaparvata lugens</i> clone NI3 carboxylesterase precursor	MF278673.1	S2
chr13.0231.t1	<i>Nilaparvata lugens</i> clone NI48 hypothetical protein	MF278715.1	S2
chr04.0145.t1	<i>Nilaparvata lugens</i> salivary sheath protein (NI33/NIShp)	KT764972.1, MF278701.1	S1
chr12.0438.t1	<i>Nilaparvata lugens</i> salivap-3/BISP (LOC111051577)	KU365937.1	S1, S3
chr05.1218.t1	<i>Nilaparvata lugens</i> trypsin-25	KJ512136.1	This study
chrX.1425.t1	<i>Nilaparvata lugens</i> phosphate carrier protein, mitochondrial-like (LOC111061302)	XM_022348996.1	This study
chr10.0094.t1	<i>Nilaparvata lugens</i> annexin A2-like protein, NI66	XM_022342235.1, MF278732.1	S2
chr03.0845.t1	<i>Nilaparvata lugens</i> profilin (LOC111049006), NISFP_unconfirmed_comp27457 seminal fluid protein	XM_022334999.1, KU932337.1	This study
chr07.0115.t1	<i>Nilaparvata lugens</i> NI1 EF-hand motif protein (LOC111055487)	MF278671.1, XM_022342702.1	S2
chr11.0447.t1	<i>Nilaparvata lugens</i> four and a half LIM domains protein 2 (LOC111051634), prickle-like protein 3 (LOC111053000)	XM_022338188.1, XM_022339830.1	This study
chr11.0142.t1	<i>Nilaparvata lugens</i> uncharacterized (LOC111052897/LOC111052895)	XM_022339709.1, XM_022339707.1	This study
chr10.0196.t3	<i>Nilaparvata lugens</i> myosin heavy chain, muscle (LOC111049488)	XM_022335714.1	This study
chr05.0533.t1	<i>Nilaparvata lugens</i> programmed cell death protein 4 (LOC111050730)	XM_022337080.1	This study
chr03.0491.t4	<i>Nilaparvata lugens</i> peptidyl-prolyl cis-trans isomerase 6-like (LOC111043670), secreted seminal fluid protein	XM_022328683.1, KU932224.1	This study
chr13.0283.t1	<i>Nilaparvata lugens</i> cathepsin B-like cysteine proteinase 4 (LOC111048658)	XM_022334589.1	This study

chr09.0212.t1	<i>Nilaparvata lugens</i> uncharacterized (LOC111055944), Arthropod defensin	XM_022343249.1	This study
chr08.1008.t1	<i>Nilaparvata lugens</i> mRNA for lipophorin precursor (NISP4), apolipophorins (LOC111049867)	AB465596.1, XM_022336048.1	This study
chr04.1268.t1	<i>Nilaparvata lugens</i> uncharacterized (LOC111064634), Chitin binding domain	XM_022352394.1	This study
chr04.0029.t1	<i>Nilaparvata lugens</i> histone H1-like (LOC111057020)	XM_022344439.1	This study
chr12.0536.t1	<i>Nilaparvata lugens</i> uncharacterized (LOC111050237)	XM_022336529.1	This study
chr06.0287.t3	<i>Nilaparvata lugens</i> heat shock 70 kDa protein (NISP1), NISFP_secreted_comp36780 seminal fluid protein	KU932222.1, XM_022337451.1	This study
chr04.1212.t1	<i>Nilaparvata lugens</i> putative inorganic phosphate cotransporter (LOC111044010)	XM_022329061.1	This study
chr09.0164.t1	<i>Nilaparvata lugens</i> trypsin-9, trypsin-like protease	AJ316142.1, KJ512120.1	This study
chr12.0385.t1	<i>Nilaparvata lugens</i> voltage-dependent anion-selective channel-like (LOC111059470)	XM_022347131.1	This study
chr05.0502.t1	<i>Nilaparvata lugens</i> apolipoprotein D-like (LOC111046805)	XM_022332442.1	This study
chrX.1656.t1	<i>Nilaparvata lugens</i> uncharacterized (LOC111053686), ATP synthase subunit gamma, mitochondrial	XM_022340604.1	This study
chr07.0132.t1	<i>Nilaparvata lugens</i> uncharacterized (LOC111054816)	XM_022341916.1	This study
chr02.0357.t1	<i>Nilaparvata lugens</i> ATP-citrate synthase-like (LOC111048221)	XM_022334091.1, XM_022334090.1	This study
chr09.0427.t1	<i>Nilaparvata lugens</i> kallikrein-6-like (LOC111044315), uncharacterized LOC111044314	XM_022329413.1, XM_022329414.1	This study

**Table S1 List of detected BPH-secreted salivary proteins, related to Figure 1.** Putative “effector proteins” are highlighted in blue.

### Supplemental References

- S1. Huang, H.J., Liu, W.C., Huang, X.H., Zhou, X., Zhuo, J.C., and Zhang, C.X. (2016). Screening and Functional Analyses of *Nilaparvata lugens* Salivary Proteome. *J. Proteome Res.* **15**, 1883–1896.
- S2. Rao, W., Zheng, X.H., Liu, B.F., Guo, Q., Guo, J.P., Wu, Y., Shanguan, X.X., Wang, H.Y.,

Wu, D., Wang, Z.Z. *et al.* (2019). Secretome analysis and in planta expression of salivary proteins identify candidate effectors from the brown planthopper, *Nilaparvata lugens*. *Mol. Plant Microbe Interact.* 32, 227–239.

S3. Guo, J., Wang, H., Guan, W., Guo, Q., Wang, J., Yang, J., Peng, Y., Shan, J., Gao, M., Shi, S., *et al.* (2023). A tripartite rheostat controls self-regulated host plant resistance to insects. *Nature* 618:799–807.